NTNU
Norwegian University of
Science and Technology

Proton therapy of head and neck cancer: evaluation of PTV-based and robust optimized IMPT versus VMAT

Anja Einebærholm Aarberg

Master of Science in Physics and Mathematics
Submission date: June 2017
Supervisor: Signe Danielsen, IFY
Co-supervisor: Sigrun Saur Almberg, St. Olavs Hospital
Jomar Frengen, St. Olavs Hospital

Norwegian University of Science and Technology
Department of Physics

Abstract

Radiation therapy for head and neck cancers has had an essential role for curative treatment for many years. Due to the location of the cancer, several critical organs will get irradiated and this may lead to serious side-effects, such as xerostomia, dysphagia and secondary malignancies. In this thesis the possible benefits of proton therapy is investigated by comparing Volumetric modulated arc therapy (VMAT) and Intensity modulated proton therapy (IMPT) for patients with oropharynx cancer. Two different techniques to achieve adequate target coverage were tried out: planning target volume (PTV)-based IMPT and robust optimized IMPT.

The IMPT plans were kept equal (or better) in terms of target dose coverage as VMAT. The mean parotid dose was then reduced as much as possible without losing target coverage. The mean dose to both parotid glands were reduced for 8 of 12 patients with a corresponding reduction in the normal tissue complication probability (NTCP). It was shown that robust optimized IMPT achieved the lowest mean parotid dose and also the lowest NTCP.

A repeat CT was taken halfway through the treatment and was used to check IMPTs robustness for patient anatomy changes. The robust optimized IMPT was deemed the most robust, where 11 of 12 patients still had adequate target coverage. For medulla the maximum dose (50 Gy) was exceeded for 1 patients for PTV-based IMPT and for none of the patients for robust optimized IMPT. For 2 patients perturbed dose distributions were made and the robust optimized IMPT plan was again deemed the most robust against set up uncertainties.

This study showed that some patients might benefit from IMPT, but for other patients VMAT may yield the same treatment effects. Robust optimized IMPT should be preferred over PTV-based IMPT.

Samandrag

Stråleterapi for hovud- og halskreft har lenge hatt ei sentral rolle for kurativ behandling. Hovud- og halsområdet har fleire kritiske organ som vil bli stråla samtidig som tumoren og dette kan føre til seriøse biverknadar, som til dømes xerostomia, dysphagia og sekundær kreft. I denne oppgåva er moglege fordelar av protonterapi sett på ved å samanlikne volumetrisk modulert stråleterapi (VMAT) med intensitesmodulert protonterapi (IMPT) for pasientar med oropharynx kreft. To ulike teknikkar for å få adekvat målvolumdekning er prøvd ut: PTV-basert IMPT og robust optimisert IMPT.

Målvolumdekninga til IMPT-planane var uendra (eller betre) samanlikna med VMAT. Gjennomsnittleg dose til parotis vart redusert så mykje som mogleg før det gjekk ut over målvolumdekninga. Den gjennomsnittlege dosen til begge parotis blei redusert for 8 av 12 pasientar, med ein tilsvarande redusering i normalvevskomplikasjonsraten (NTCP). Det blei vist at den robust optimaliserte IMPT-planen oppnådde dei lågaste gjennomsnittsdosane og NTCP-verdiar.

Ein ny CT blei tatt halvvegs i behandlinga og blei brukt til å sjekke robustheita til IMPT for endringar i pasientanatomi. Robust optimaliserte IMPT blei ansett for å vere den mest robuste, med målvolumdekning for 11 av 12 pasientar. For medulla var det 1 pasient som fekk over 50 Gy for PTV-basert og ingen for robust optimalisert IMPT. Perturberte doseplanar blei laga for 2 pasientar og den robust optimaliserte IMPT-planen var igjen sett som den mest robuste.

Denne oppgåva viser at nokre pasientar vil ha fordel av behandling med IMPT, medan VMAT gir same behandlingseffekt for andre pasientar. Robust optimalisering bør veljast over PTV-baset IMPT.

Preface

This master thesis is written as the conclusion of my study of Biophysics and Medical Technology at the Norwegian University of Science and Technology (NTNU). The work was done in the spring of 2017 at the Department of Radiotherapy at St. Olavs Hospital.

I would like to thank my supervisor at St. Olavs Hospital, medical physicist Sigrun Saur Almberg, for valuable help and guidance throughout the entire project work and writing process. I would also like to thank co-supervisor Jomar Frengen for advice during the practical work of this thesis. My supervisor at NTNU, Signe Danielsen, deserves a thanks, for the advice, feedback and encouragements given in the writing process of this master thesis.

A special thanks to Torbjørn Furre at Radiumhospitalet. And thank you, Liv Grønli Turtum, for the encouragements throughout and proof-reading at the end.

Anja Einebærholm Aarberg
Trondheim, June 2017

Table of Contents

Acronyms

CT Computed tomography

CTV Clinical target volume

DVH Dose volume histogram

EUD Equivalent Uniform Dose

GTV Gross tumor volume

HU Hounsfield Unit

ICRU International Commission on Radiation Units and Measurements

IMPT Intensity Modulated Proton Therapy

IMPT-PTV Planning target volume-based IMPT

IMPT-Robust Robust optimized IMPT

IMRT Intensity Modulated Radiation Therapy

ITV Internal target volume

KVIST Kvalitetssikring i stråleterapi

LET Linear energy transfer

LINAC Linear Accelerator

LKB Lyman-Kutcher-Burman

NRPA Norwegian Radiation Protection Authority (Statens strålevern)

NTCP Normal tissue complication probability

OAR Organs at risk

PTV Planning target volume

RBE Relative biological effectiveness

SFUD Single Field Uniform Dose

SOBP Spread-out Bragg Peak

TCP Tumor control probability

VMAT Volumetric modulated arc therapy

Chapter 1

Introduction

Head and neck cancers include cancers of the mouth, lips, throat, nose, larynx and salivary glands. In 2015 there were 774 new cases in Norway, corresponding to 2% of all new cancer cases (1). The main portion of these are diagnosed with squamous cell carcinoma with the primary tumor site often seen in the mucosa of the upper aeordigestive tract. The treatment of choice (and prognosis) depend on the location and the probability of tumor spreading (2).

Head and neck cancers can be treated with surgery, chemotherapy and/or radiation therapy. A combination of these are commonly needed for curative treatment and often also given for palliative treatment. Techniques for photon radiation therapy used today are mainly Intensity Modulated Radiation Therapy (IMRT), and a variant called Volumetric Modulated Arc Therapy (VMAT) (3), which have resulted in better dose distribution and improved outcomes compared to earlier radiation therapy techniques (4). Nevertheless, the treatment of head and neck cancer is still associated with several side-effects because the target volumes are located close to several organs at risk. Examples of side-effects are: xerostomia, dysphagia, neck fibrosis, esophageal stenosis, hearing impairment, optic neuropathy, temporal lobe necrosis and secondary malignancies (5).

Protons exhibit favorable properties for radiation therapy, they have finite range and the prospect of delivering higher dose to the tumor without increasing the dose to the surrounding healthy tissue. This may lead to sparing of normal tissues and organs at risk in the head and neck cases (6). As a result of this several proton centers have begun giving proton therapy for head and neck patients. One major problem that has presented itself is which patients benefit from pro-

ton therapy and this led to a group in the Netherlands introducing a model-based approach for selecting patients who would likely benefit from Intensity Modulated Proton Therapy (IMPT) based on normal tissue complication probability (NTCP) calculations (7).

A concern regarding IMPT, is that it is thought to be severely affected by uncertainties including anatomical changes, patient setup errors and range uncertainties (8). There are two approaches for taking setup errors and range uncertainties into account today; either add a geometrical margin to the target volume or apply robust optimization. The former is common for photons, but is thought not to be adequate for proton therapy (9). Methods of robust optimization seek to incorporate setup and range uncertainties in the treatment optimization by adding a number of different possible scenarios to the optimization problem (10; 11). For head and neck cancer patients, weight loss and shrinking of tumors during treatment are common, which can lead to poor dose coverage of target volumes or increased dose to organs at risk. Adaptive radiotherapy is suggested to account for this, and involves taking new CT scans for re-planning throughout the course of the treatment (12).

In this master thesis the main focus has been to investigate the possible benefits of proton therapy for head and neck cancers. The aims were:

1. Find suitable treatment parameters for IMPT of oropharynx cancer, including field numbers, angles and some standardized optimization criteria.
2. Investigate the potential in IMPT compared to VMAT for oropharynx cancer patients.
3. Investigate the robustness of the IMPT plans by recalculating the plans on CT scans taken halfway through the treatment.

12 patients treated for oropharynx cancer at St. Olavs Hospital during 2016 were included in the study.

Chapter 2

Theory

The following chapter is in part based on and adapted from the authors project work in the fall of 2016: ”Comparison of 3D-CRT, VMAT and Proton Therapy of Mediastinal Lymphoma” (13).

2.1 Physics of radiation

Ionizing radiation is radiation that transfer sufficient energy to cause ionizations and excitations in the medium it penetrates. The energy transfer is due to various atomic and nuclear interactions, which will slow down and/or change the direction of the primary particle track. Photons and neutrons are indirectly ionizing radiation because they release secondary particles in the medium, which in turn causes ionizations. Charged particles are directly ionizing radiation because they transfer the energy directly from the charged particle to the medium. (14)

2.1.1 Absorbed dose

To quantify the energy deposited in the medium the absorbed dose (D) is defined as the average amount of energy imparted ($d\varepsilon$) per unit mass (dm) of the irradiated medium (15):

$$D = \frac{d\varepsilon}{dm}. \tag{2.1}$$

The absorbed dose is measured in Gy ($\mathrm{J\,kg^{-1}}$).

2.1.2 Photon interactions

A photon beam hitting a medium will be attenuated due to interactions. The attenuation of a photon beam in matter is described by

$$I(x) = I_0 e^{-\mu x}, \tag{2.2}$$

where I_0 is the intensity of the photons before hitting the medium and I is the intensity of the photons after passing a length, x, of the medium with a linear attenuation coefficient, μ (14). μ is the probability of interaction per unit length and is dependent on the photon energy and the atomic number of the medium.

Photons mainly interact with matter in three ways for therapeutic energies; photoelectric effect (PE), Compton scattering (C) and pair production (PP). All of which result in the release of secondary electrons that cause energy deposition in a medium. The total mass attenuation coefficient is the probability of interaction (per unit length and mass) and is defined as

$$\frac{\mu}{\rho} = \frac{\mu_{PE}}{\rho} + \frac{\mu_C}{\rho} + \frac{\mu_{PP}}{\rho}. \tag{2.3}$$

For external radiation therapy the energies range from 0.1 to 20 MeV and for these energies the Compton scattering probability is dominating. Compton scattering depends on the electron density of the medium, but is nearly independent of atomic number. The result of the interaction is a photon with less energy than the primary photon and an electron. (14)

Interactions attenuate the photon beam, however not all photons will interact within the patient. A portion of the photons will go straight through the patient without much energy loss. Photons interact indirectly and this creates a build-up region, corresponding to the electron range, for the dose as a function of depth. This is illustrated in figure 2.1 for the depth-dose curve of a 10 MV photon beam (in blue).

2.1.3 Proton interactions

Protons, here defined as heavy charged particles, interact with a medium in three different ways: stopping, scattering and nuclear interactions.

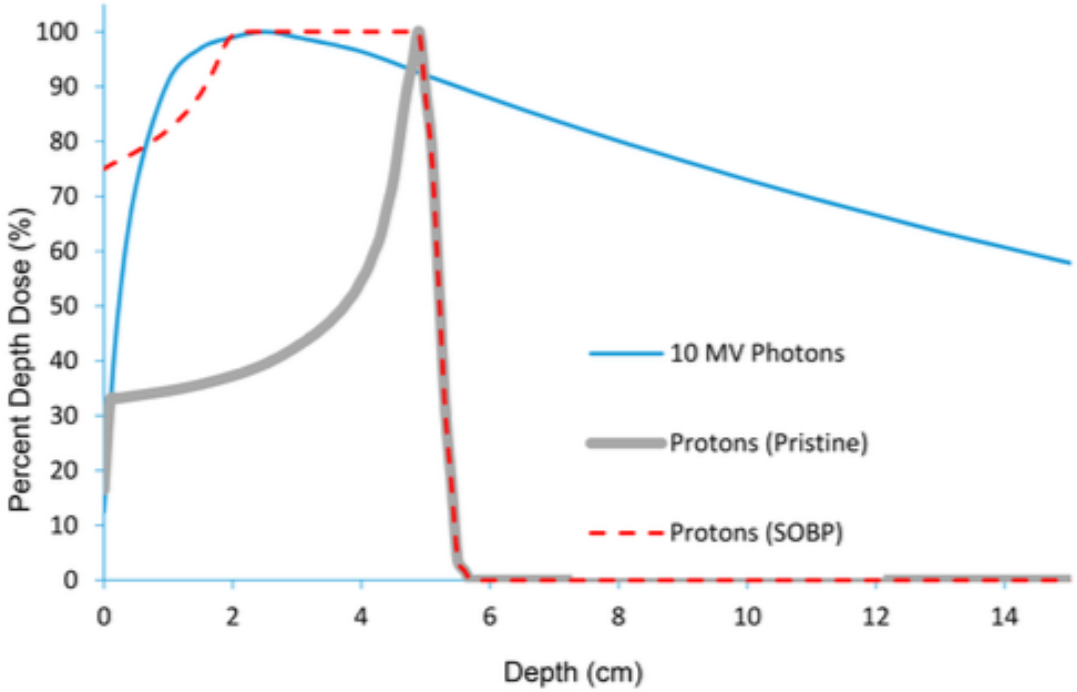

Figure 2.1: The depth-dose curve for photons (blue line), pristine protons (grey line) and spread-out Bragg peak (SOBP) protons (red dotted line). It clearly shows a build up region and slow dose fall off for the photons and the Bragg Peak, and rapid dose fall off for the protons. The illustration is borrowed from (16).

Stopping

A charged particle will slow down in the medium by colliding with atomic electrons along its path. The particle loses more energy the longer it interacts with the electrons, which means that the amount of energy transferred depends on the velocity and charge of the particle, and density of the medium. These energy losses can be described by the stopping power, defined as the average energy loss, dE, per unit distance, dx, along the particle track in a medium (14).

The Bethe-Bloch formula gives a theoretical description of the stopping of heavy charged particles through matter:

$$-\frac{dE}{dx} = \left(\frac{ze^2}{4\pi\varepsilon_0}\right)^2 \frac{4\pi Z\rho N_A}{Am_e v^2}\left[\ln\left(\frac{2m_e v^2}{I}\right) - \ln(1-\beta^2) - \beta^2\right], \tag{2.4}$$

where the different parameters and a description of these are found in table 2.1 (17). From equation 2.4 it can be seen that the stopping power is inversely proportional to the velocity of the particle squared, which explains the Bragg Peak for charged particles.

Table 2.1: Parameters and description in the Bethe-Bloch formula for the stopping power of heavy charged particles.

Parameter	Description
ze	Charge of the incident particle
m_e	Electron mass = 0.511 MeV/c^2
N_a	Avogadro's number = $6.022 \cdot 10^{23}$ mol^{-1}
I	Mean energy required to ionize an atom in the medium
Z, A	Atomic number and atomic weight of the absorber medium
ρ	Material density
β	v/c of incident particle

For a proton beam it will be a prominent peak (the Bragg Peak) at a depth, depending on the protons energy. This is because the proton deposits more dose as it slows down and as it nearly stops it deposits the rest of the energy within a small area, as seen in figure 2.1 (in grey). This figure also shows a spread-out Bragg Peak (SOBP) in red, which is created by summing the depth doses from protons of different initial energy. A SOBP is used clinically to cover the target volume.

Scattering

A proton incident on a medium will also collide with atomic nuclei, and because both the proton and the nuclei are positively charged, the proton (much smaller mass than the nucleus) will deflect from its path. The scattering angle from one such collision is very small and therefore negligible, but after several collisions the scattering might be considerable. The summation of all of these small deflections is a statistical observation and is often called multiple Coulomb scattering (18).

Nuclear interaction

In addition to stopping and scattering, the proton may collide head-on with the atomic nucleus in the medium. This effect is not prominent but has to be considered when dealing with proton beams. When the proton collides with the nucleus, fragments of the nucleus will be set in motion. These fragments may be protons, neutrons, electrons or larger fractions of the nucleus. The fragments tend to have lower energies and deposits dose just downstream of the reaction site before they stop. (18)

2.1.4 LET and RBE

Linear energy transfer (LET) is defined as the average energy locally imparted to the medium by a charged particle of specified energy in traversing a distance in that medium (15). LET has the unit $\mathrm{keV\,\mu m^{-1}}$ and describes the density of ionization's along the particles path. High-LET radiation are densely ionizing radiation such as energetic neutrons, proton and other heavy charged particles. Low-LET radiation are sparsely ionizing radiation, such as photons. The high-LET radiation will produce more cell killing per Gy, but for very high-LET ($\mathrm{LET} > 100\,\mathrm{keV\,\mu m^{-1}}$) radiation the cell killing is less efficient. This is due to overkill, which means that the radiation waste energy on cells that are already dead and therefore there is less likelihood per Gy that other cells in the tissue will be killed (19). For protons the LET will increase as the energy deposited to the medium increases, i.e. the LET increases as the beam pass through the medium.

For different radiation qualities the effect of the absorbed dose is not necessarily the same: biological effects must also be taken into account. The relative biological effectiveness (RBE) is defined as:

$$\mathrm{RBE} = \frac{\text{dose of reference radiation}}{\text{dose of test radiation}}, \tag{2.5}$$

where the test refers to the radiation quality that is to be compared to the reference radiation quality (19). The reference beam is usually low-LET 250 kVp X-rays (19), but Cobolt-60 rays (1.25 MeV) are also used (20). The RBE vary with radiation quality, but also with fractionation, cell type and dose rate. Protons are slightly more biologically damaging than photons and the RBE mostly depends on LET. The RBE of the protons depend slightly on depth and will be highest at the Bragg peak (21). Even so, a constant RBE of 1.1 is usually set for protons used clinically (22). The value of 1.1 is based on experiments done in the 1950's and seems to be a reasonable constant value for clinical beam energies (21).

2.2 Generation of a clinical radiation beam

2.2.1 Photon beam

The most commonly used radiation quality in therapy today is photons, created by a linear accelerator (linac). In a linac, electrons gain energy by interacting with a synchronous radio-

frequent electromagnetic field before bending and hitting a target (14). The interaction between electrons and the target releases photons (bremsstrahlung). A schematic drawing of a linac can be seen in figure 2.2. The photon beam can be shaped by collimators to hit an area of choice, such as a tumor.

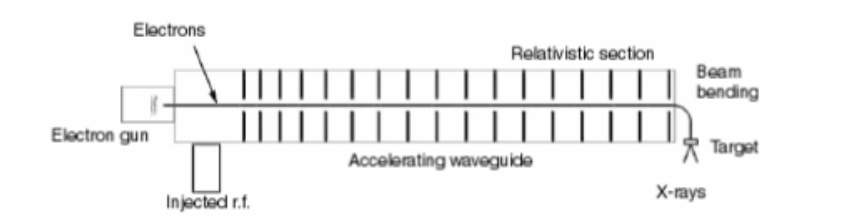

Figure 2.2: A schematic drawing of a linear accelerator used for photon based radiation therapy. The electrons interact with a electromagnetic field in the accelerating waveguide before hitting a target and producing photons (14).

The introduction of modern techniques for treatment planning and delivery, i.e. IMRT, of head and neck cancer has decreased the toxicities associated with radiation therapy, and also in many cases increased the local control of the cancer (3). IMRT is a technique that produces conform dose distributions by varying the intensity of the radiation beam during treatment, illustrated in figure 2.3a. Also seen in figure 2.3b is an example dose distribution of a head and neck treatment plan using IMRT.

IMRT is applied to complex target volumes to conform the distribution to the target volume and limit the dose to nearby organs at risk. In IMRT, multiple non-uniform radiation fields are used and shaped according to the projection of the target volume, taking into consideration dose-volume objectives of the surrounding volumes. IMRT is an iterative technique which utilizes inverse planning; the user defines constraints and objectives, which the iteration algorithm will take into consideration to solve the treatment planning problem. (23)

VMAT

Volumetric modulated arc therapy (VMAT) is a variant of the IMRT-technique were the gantry moves continuously around the patients while the dose rate and field shape vary with the position of the gantry (24). The treatment can be delivered in one or more arcs, depending on the location and complexity of the tumor. Typically, a checkpoint every $\sim 4^{\circ}$ ensures proper dose

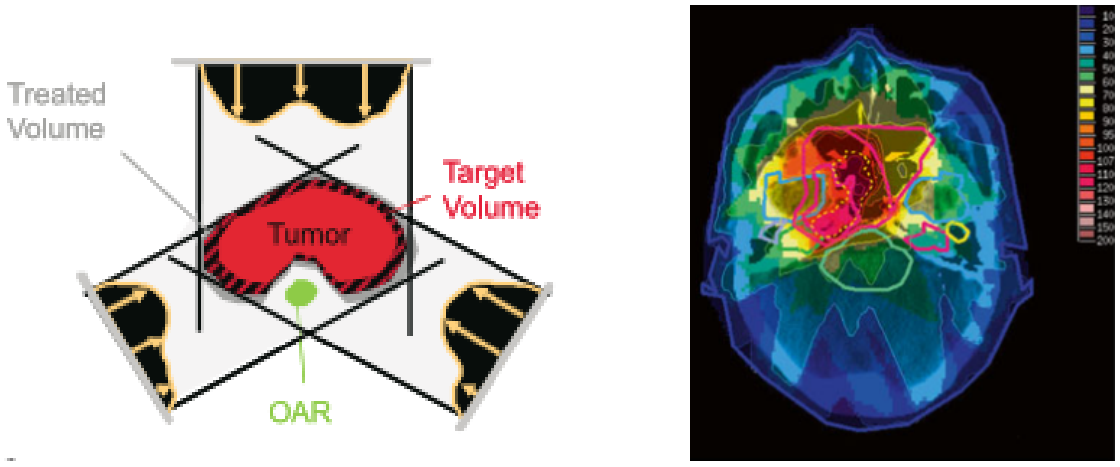

(a) (b)

Figure 2.3: IMRT, (a) schematic drawing of intensity modulation (23) and (b) an example dose distribution (24) for a head and neck case.

delivery. The main advantage of VMAT over IMRT is the speed of treatment delivery; typically 2-3 minutes for VMAT versus 10-20 minutes for IMRT. (20)

2.2.2 Proton beam

To accelerate protons to clinical beam energies to reach the desired depths either a cyclotron or a synchrotron is used. As the cyclotron is the most common among clinical installations it will be briefly described here.

Cyclotrons accelerate protons to a fixed energy that are modulated with a degrader to deliver the intended energies to the patient. It is a short metallic cylinder consisting of two metal electrodes, called dees, where a varying electric potential will accelerate the incoming charged particle. A magnetic field is set up perpendicular to the electric field so that the particle spirals out towards the edge of the dees when its energy is increased (20). Combining the Lorentz force, $F_B = qvB$, and the centripetal force for non-relativistic particles, $F_C = \frac{mv^2}{r}$, gives

$$qvB = \frac{mv^2}{r}$$

$$v = \frac{qBr}{m}.$$

The kinetic energy of the particle, $E = \frac{mv^2}{2}$, can thus be written as

$$E = \frac{(qBr)^2}{2m}. \tag{2.6}$$

The maximum particle energy depends on the radius of the electrodes of the cyclotron and the strength of the magnetic field, B. The maximum energy for a cyclotron is about 250 MeV and when the particle reach this energy it is ejected and transported towards the treatment room (20).

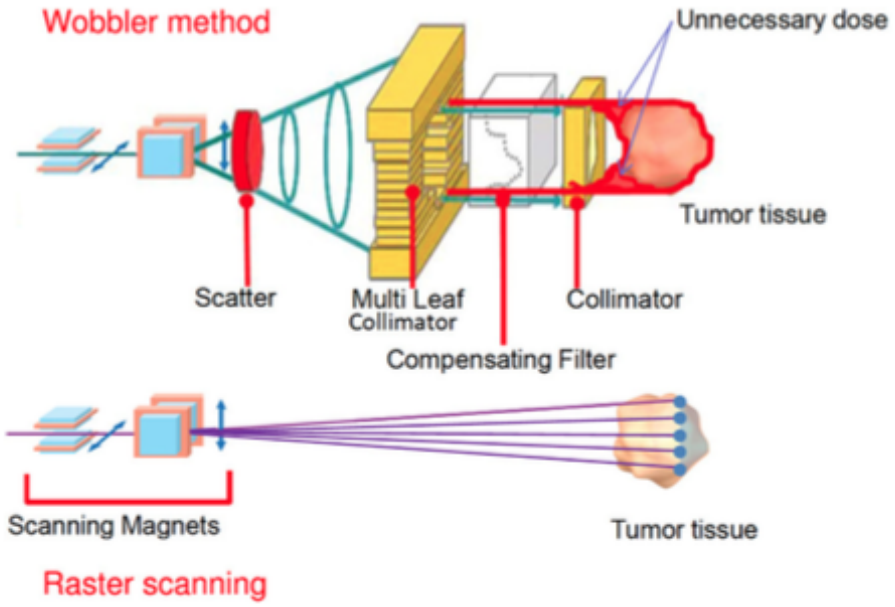

Figure 2.4: Example of possible setup for (top) passive scattering and (bottom) active scanning (25).

There are two methods of delivering proton therapy: passive scattering and active scanning (26). Passive scattering use materials with high atomic numbers to scatter the beam to usable lateral dimensions and then modulate the energy creating a so called spread out Bragg Peak (SOBP) to cover the desired depth, as seen in figure 2.4 (top). Active scanning or beam scanning is a technique that deflects the beam across the target by moving the pencil beam, as illustrated in figure 2.4 (bottom). The beam is usually steered by magnets that deflect the beam so that the whole target can be covered. Active scanning is used for a technique called single field uniform dose (SFUD) where individually optimized pencil beams from each field delivers a homogeneous dose to the target volume. The goal is to deliver a dose distribution across the target that is as homogeneous as possible (26).

Active scanning can deliver intensity modulated proton therapy (IMPT), analogous to IMRT for photons, by varying the fluence in each spot of the scan and/or the beam intensity. The dose can be delivered non-uniformly on a field-by-field basis, and add up to a uniform target

dose. IMPT simultaneously optimizes the pencil beams from all the fields. Each field may not be homogeneous across the target but the dose distribution from all fields will still be homogeneous. IMPT place the Bragg peaks throughout the target volume and give them adjusted weights across the target, as homogeneously as possible (26). Although passive scattering has been used the longest, the use of active scanning techniques are increasing, and are considered to be the future of proton therapy.

Proton planning for head and neck cancer today

IMPT is currently being used in several proton centers around the world to treat head and neck cancer. Two well-recognized centers are MD Anderson and the Paul Sheffer Institute (PSI). They use different field arrangements clinically, and below is a brief summary of both.

MD Anderson use a three field configuration; two anterior oblique beams ($\pm 50^\circ - 70^\circ$) and one posterior beam (180°), illustrated in figure 2.5a. They also use a couch angle for the anterior beams of $15^\circ - 20^\circ$. This is done to optimize the target coverage and minimize the dose to unnecessary tissue and organs at risk (OAR). Another reason for this choice is to reduce uncertainties in proton range by avoiding irradiating through the mouth. (27)

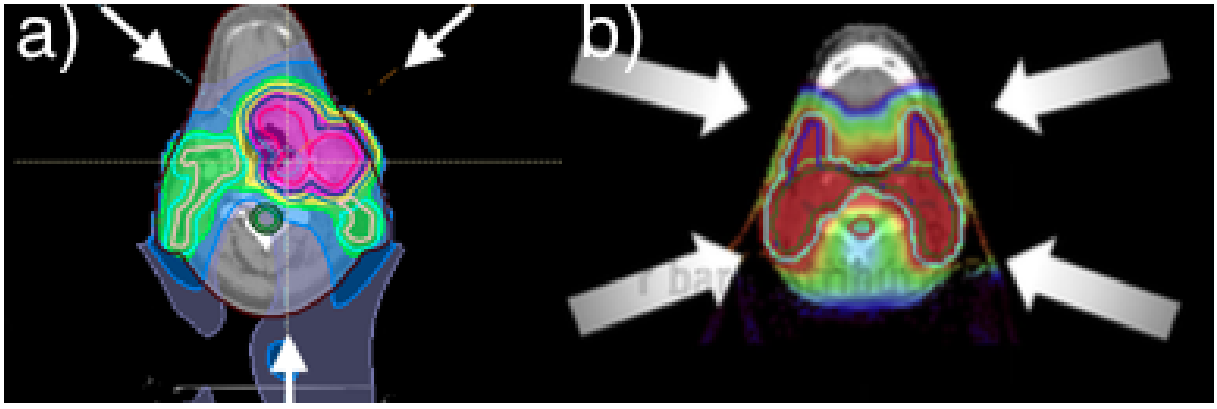

Figure 2.5: a) Snapshot showing MD Anderssons field configuration and b) figure from (28) showing the field configuration used at PSI.

PSI use a 4 field star-technique, as seen in figure 2.5b, using two anterior, oblique ($\pm 60^\circ$) beams and two posterior oblique ($\pm 100^\circ$) beams to deliver the prescribed dose. The reason for this is to provide robust coverage of the target volumes. (28; 29)

2.3 Treatment planning

2.3.1 CT

To begin treatment planning the anatomy of the patient is imaged by a CT scan. The unit used in CT is Hounsfield unit (HU) and is defined as:

$$\mathrm{HU} = 1000 \cdot \frac{\mu - \mu_{water}}{\mu_{water}}, \tag{2.7}$$

where μ is the linear attenuation coefficient, and HU = -1000 for air and HU = 0 for water. It is common to use a mass density of $0.001\,21\,\mathrm{g/cm^3}$ for all HU values less than -1000 and a mass density of $7.87\,\mathrm{g/cm^3}$ for HU above 2800 (30).

For treatment planning the HU numbers are converted into electron mass densities that can be used to identify the different tissues in the patient. A snapshot from RayStation (RaySearch Laboratories) illustrates this relationship in figure 2.6. For proton therapy the HU numbers are converted into proton stopping power values using a calibration curve (18). Errors in the HU numbers will therefore translate into uncertainties in the range of protons. A CT with high precision is needed for proton therapy in order to minimize the range uncertainties.

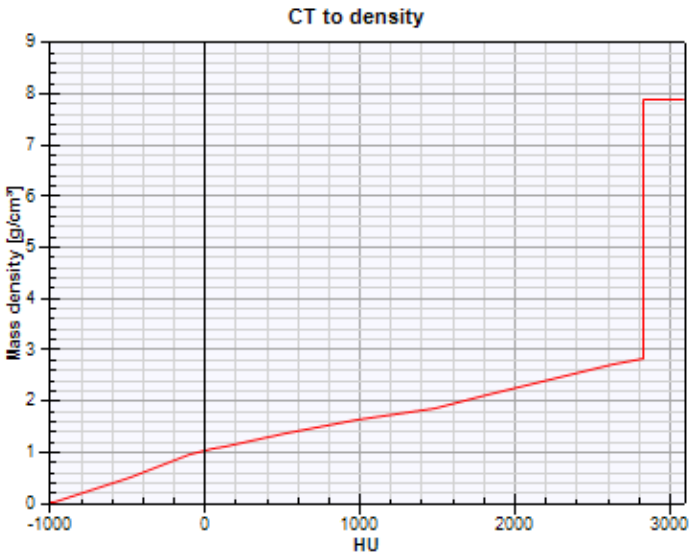

Figure 2.6: CT Hounsfield units to density conversion graph, taken from RayStation interface (30).

As any imaging modality, CT is prone to artifacts. An example of metal artifacts is shown in figure 2.7. CT image reconstruction is performed using a filtered back projection method, which

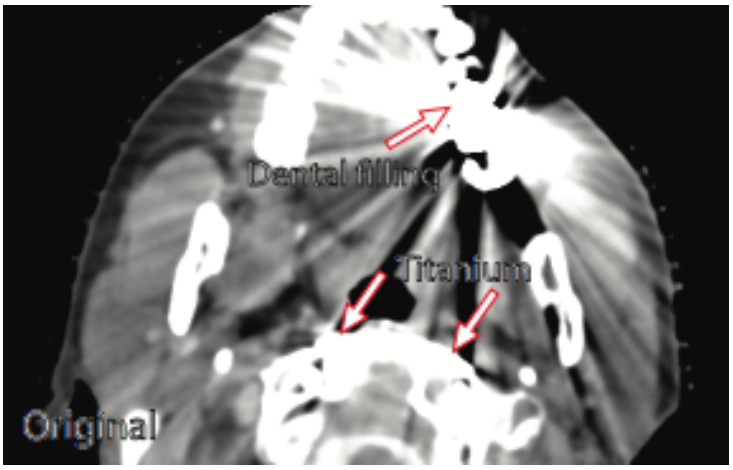

Figure 2.7: Example CT scan from a patient with titanium implants in the cervical spine and dental fillings, image from Verburg and Seco (31).

assumes monochromatic x-ray attenuation and a complete set of projection measurements (31), and can result in artifacts. The metal artifacts can have great impact on the dose calculation and should be taken into account when making treatment plans.

2.3.2 Volume delineation

Volume structures are delineated on the CT images by a physician before any treatment planning can be done. A region of interest (ROI) is usually either a target or an organ at risk (OAR). The following description of the ROIs are based on the KVIST-group report form the Norwegian Radiation Protection Authority (NRPA) (32), which again is based on ICRU report 83 (33).

Target volumes

The target volumes are divided into several areas with different margins to account for uncertainties, as can be seen in figure 2.8. The gross tumor volume (GTV) is the solid or demonstrable tumor one can identify from the images taken. The clinical target volume (CTV) is the GTV with margins that account for sub-clinical spread in the tissue and involvement of elective areas. This is the volume that should be treated. The internal target volume (ITV), takes the uncertainties in position of the CTV in the patient into account. Around the CTV (or ITV), a planning target volume (PTV) is delineated to take into account patient motion and uncertainties in setup and delivery of the treatment. The PTV is used to ensure that the prescribed dose actually is delivered to the CTV.

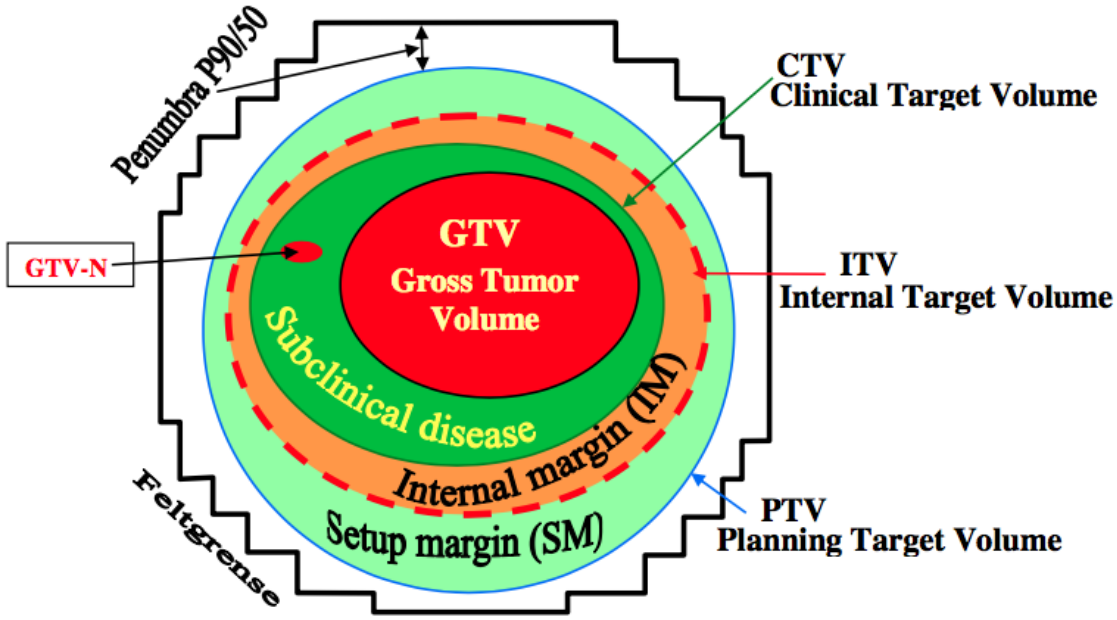

Figure 2.8: Illustration of target volumes and margins defined by the KVIST-group (32).

Risk volumes

Organs at risk (OAR) are delineated to ensure that radiation sensitive tissue, that may limit the treatment plan, are taken into account. A planning organ at risk volume (PRV) are often added for serial organs in the same way as a PTV is added to the CTV to take into account uncertainties. All tissues could be regarded as OAR as irradiating healthy tissue is known to enhance the risk for late radiation effect, but usually only organs with critical function close to the CTV are delineated.

Patient uncertainties in proton therapy

IMPT is thought to be heavily affected by uncertainties because of the precision in which the beam is delivered and the conformity of the dose distribution (steep gradients of the pencil beams). The most prominent uncertainties are anatomical changes, patient setup errors and range uncertainties. The anatomical changes can be organ motion, changes in the sinuses (air cavities), tumor volume increase/decrease and/or patient weight loss or gain. The range uncertainties come from uncertainties regarding the Hounsfield units (HU) used for the images taken with computed tomography (CT) and the conversion between HUs into stopping power for protons. (8)

To account for uncertainties in photon radiation therapy a planning target volume (PTV) is usually made from the clinical target volume (CTV). The margin between the PTV and the CTV is determined based on setup errors and tumor movement, since range uncertainties in photons are of far less importance than for protons. In the literature today several articles do not recommend the use of a PTV for protons (9; 11; 34; 35) and they suggest instead the use of a robust optimization method to account for both setup error and range uncertainties. Methods have been proposed in several articles (11; 34; 36) and the robust method is now regarded by many as the best way to make the proton treatment plans robust against uncertainties.

2.3.3 Plan optimization

Inverse planning

Inverse planning is an optimization technique where the user defines different criteria for a treatment plan, and lets the optimizer find the best solution to the problem. The objective function can be defined as:

$$F(x) = \sum_{\sigma=1}^{S} \lambda_\sigma (D^\sigma - d^\sigma)^2 \tag{2.8}$$

$$D^\sigma = A^\sigma x \qquad \sigma = 1, ..., S; \qquad x \geq 0,$$

where σ defines the structure (i.e., an OAR or a target volume), λ_σ is a structure-specific weighting factor, D^σ is the calculated dose and d^σ is the prescribed dose, A^σ is the dose kernel matrix and x is the intensity of the beam (37). The goal of inverse planning is to minimize the objective function, e.g. find the global minimum.

A robust optimization method

One way of implementing robust optimization is to use a minimax optimization, where the optimization functions are selected to minimize the objective function in the worst case scenario (11). This gives a threshold for how much the treatment plan quality can deviate due to errors. The worst case scenario is a realization of uncertainty under which a robust function attains its highest value. For several functions, n, the minimax optimization can be formulated as

$$\min_{x \in X} \max_{s \in S} \sum_{i=1}^{n} w_i f_i(d(x;s)), \tag{2.9}$$

where X is the set of feasible variables and S is the scenarios included in the optimization. $d(x;s)$ is the dose distribution as a function of the variables x and the scenario s (11). With this method the information about the uncertainties and errors are incorporated into the optimization and it enables the treatment planning system to determine where to deposit dose to achieve plans that are robust against setup error and range uncertainties.

Practical plan optimization

In a treatment planning system the above is implemented and the user defines objectives for the target volumes and organs at risk. Examples of objectives are minimum dose to the target volumes, mean dose to a volume and/or maximum dose to an organ at risk. When the objectives are decided the weighting can be modified so that the most important, often target coverage, has the highest weight and thus has precedence over other volumes. The plan can then be iterated until the user is satisfied with the dose distribution and the treatment plan can be administered to the patient.

2.4 Plan evaluation

2.4.1 Dose volume histogram

A dose volume histogram (DVH) is a representation of radiation dose as a function of volume. A cumulative DVH show the volume elements receiving at least a given dose value (33). Illustrated in figure 2.9 and relevant to the plan evaluation process is the different D_V parameters that describe the minimum dose to a volume, V. Another parameter is V_D, which is the volume receiving a dose greater or equal than D. A parameter often used for the minimum dose value in a dose distribution is D_{98}, this is the dose at least 98% of the volume receives. For the maximum dose value D_2 is often reported, that is the dose that maximum 2% of the volume receives.

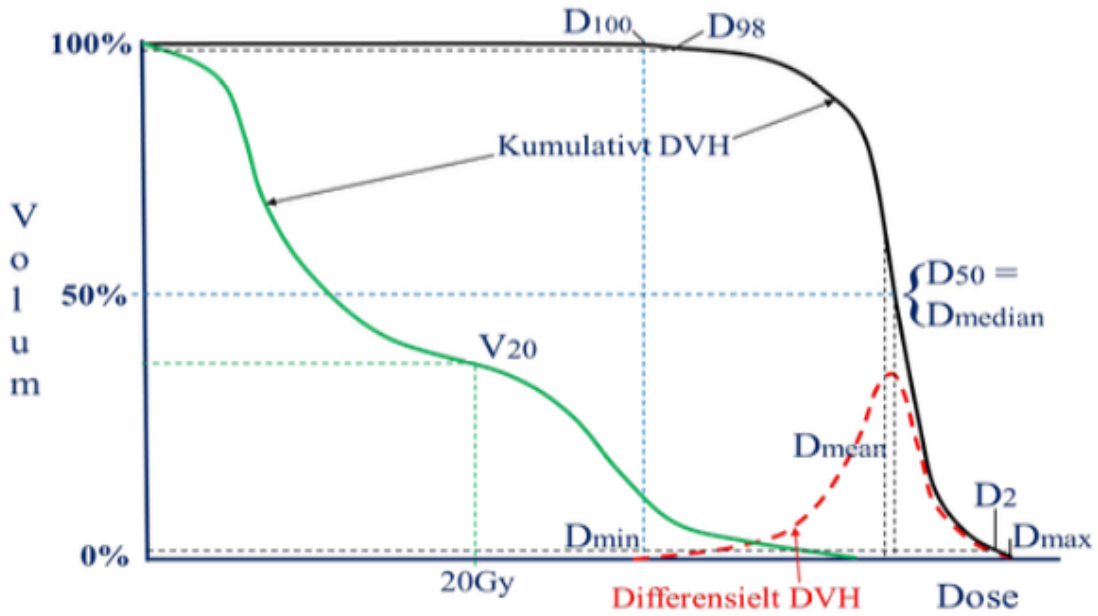

Figure 2.9: Example of DVH and parameters associated with treatment plan evaluation (32). Black: target volumes and green: organs at risk.

2.4.2 NTCP modeling

To visualize the goal of radiation therapy; to deliver enough dose to the tumor and as low dose as possible to the surrounding tissue, a helpful parameter is the therapeutic ratio. The therapeutic ratio is defined as the ratio between the tumor control probability (TCP) and the normal tissue complication probability (NTCP) at a given level of response. It can be illustrated as in figure 2.10, where curve A is the TCP and curve B is the NTCP. The goal is to have the NTCP curve as far to the right of the TCP curve as possible and thus achieve the greatest therapeutic ratio. The therapeutic ratio depends on fractionation, treatment time and technique, target volume, LET and dose rate (38).

LKB model

NTCP models are a tool for treatment plan evaluation, where the main idea is to estimate the probability for normal tissue complications from the DVH given by the treatment planning system. A frequently used NTCP-model is the Lyman-Kutcher-Burman (LKB) model (39; 40).

To report non-uniform dose distribution the equivalent uniform dose (EUD) was introduced in 1997 by Niemierko (41). The EUD assumes that two dose distributions are equivalent if the radiobiological effect is the same and is given by

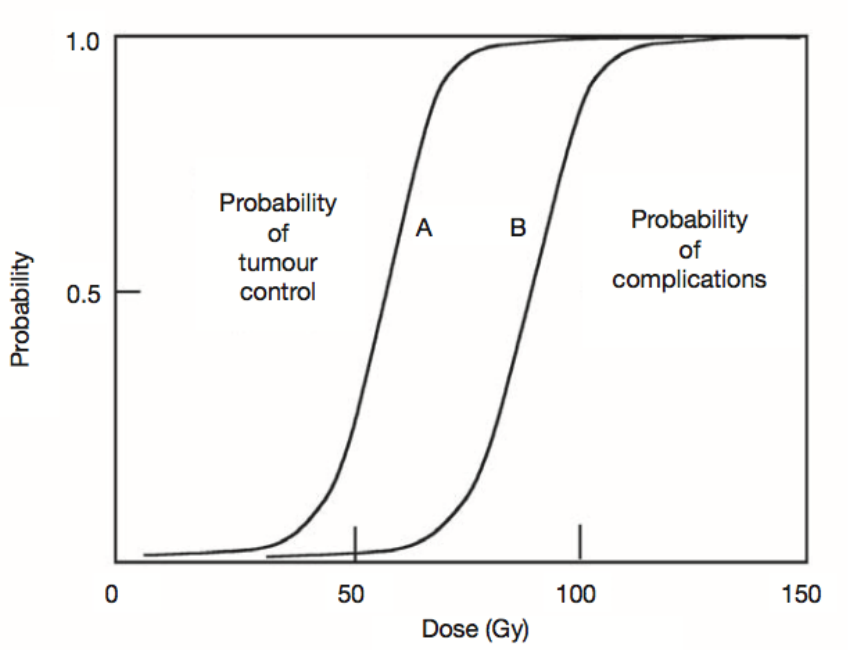

Figure 2.10: Illustration of curves for A: tumor control probability (TCP) and B: normal tissue complication probability (NTCP). The therapeutic ratio can be found by the ratio of TCP and NTCP at a specified dose (38).

$$\text{EUD} = \sum_i (D_i{}^a v_i)^{1/a}, \tag{2.10}$$

where D_i is the dose to voxel i and v_i is the relative volume of the voxel. a is a tissue-specific parameter that is determined by comparing tumor and normal tissue response. For serial organs a has a large value while for parallel organs it is closer to 1 (42).

The LKB model is an empirical NTCP model and use a cumulative Gauss function to characterize the NTCP. Mohan et. al (43) proposed a mathematical representation of the NTCP curve, which begins with an integral of the normal distribution

$$\text{NTCP} = \frac{1}{\sqrt{2\pi}} \int_{-\infty}^{t} e^{x^2/2} dx \tag{2.11}$$

where

$$t = \frac{D - TD_{50}}{mTD_{50}}, \tag{2.12}$$

m describes the steepness of the NTCP-curve and TD_{50} is the dose corresponding to a NTCP of 50%. D is given by

$$D = \sum_i (D_i{}^{1/n} v_i)^n \tag{2.13}$$

and is thus equal to the EUD when $n = 1/a$. The parameters needed for calculating NTCP using the LKB model is TD_{50}, n and m. The parameters are empirically derived by fitting the NTCP predictions for an endpoint to data from clinical outcomes for a population of treated patients (44).

2.4.3 Homogeneity index and conformity index

The homogeneity index (HI) characterizes the homogeneity of the dose within the target volume (33). In RayStation (30) it is defined as:

$$\text{HI} = \frac{\text{D(x)}}{\text{D(100-x)}}, \tag{2.14}$$

where D(x) is the dose at x% of the volume. A homogeneity index of 1 indicates a completely homogeneous dose distribution over the entire target volume.

The conformity index (CI) gives an indication of how conform the dose to the target volume is and is in RayStation (30) defined as:

$$\text{CI} = \frac{V_{\text{target volume}}}{V_{\text{treated volume}}}, \tag{2.15}$$

where $V_{\text{target volume}}$ is the volume of the delineated target volume (often the PTV) and $V_{\text{treated volume}}$ is the volume covered by a total isodose volume, where the 90% or 95% isodose is the most common to use. A conformity index near 1 indicates good conformity. A shortcoming of the CI is that it does not take into account the degree of spatial intersection of the volumes or their shapes (45). The CI can therefore be 1 without the volumes being similar or in the same area. It is therefore important to use this index in addition to visualization tools for the dose distribution, so that the risk of a total miss is minimized.

2.4.4 Robust evaluation

A method to evaluate the robustness of a treatment plan is to do a geometric shift of the isocenter, recalculate the plan and evaluate the resulting dose distribution. In a similar manner, the CT densities can be changed and the effect evaluated after re-calculation.

Chapter 3

Method

3.1 Patients

The patients in this master thesis were included in a previous project at St. Olavs Hospital. The project investigated the need for re-planning of VMAT plans for head and neck cancers based on an extra CT exam taken after 18 fractions. To be included in the original project patients had to get curative radiation treatment for head and neck cancer at St. Olavs Hospital, and lymph nodes had to be included in the radiation field, receive at least a dose of 60 Gy and have adequately cognitive function. The patients provided informed consent and the study was approved by REK (2015/2022). A subgroup of patients with oropharynx cancer from the study was selected for this master thesis.

In total 12 patients with oropharynx cancer were included in the present study. Patient information is given in table 3.1. The mean age was 61.3 years old (range: 55-79) and the staging of the cancer ranged from T2 to T4, local nodal involvement was common and none of the patients had metastases. The repeat CT was normally taken at the 18. treatment fraction, that is after 36 Gy. All plans, VMAT, PTV-based IMPT (IMPT-PTV) and robust optimized IMPT (IMPT-Robust), were made in RayStation v.5.0. The treatment machine used for VMAT was Agility Thr_feb and for IMPT the machine RSL_IBA_UNI was used.

Table 3.1: Information about the patients included in the present study.

Study #	Gender	Age	Primary tumor	TNM stage	Dental fillings
1	Male	63	Tonsil	T2N0M0	No
2	Female	61	Tonsil	T4aN2bM0	Yes
3	Male	59	Base of tongue	T1N2aM0	Yes
4	Male	55	Tonsil	T4aN2cM0	Yes
6	Male	79	Tonsil	T4aN2bM0	Yes
9	Female	62	Tonsil	T1N2aM0	No
13	Female	57	Base of tongue	T4aN0M0	Yes
18	Male	60	Tonsil	T2N2bM0	Yes
19	Male	67	Tonsil	T2N2bM0	Yes
20	Male	55	Tonsil	T2N2bM0	Yes
21	Male	56	Tonsil	T2N2bM0	No
23	Male	62	Tonsil	T2N2bM0	Yes

3.2 Treatment planning

The clinical target volumes were divided into three: a high risk volume to receive 68 Gy (CTV68), a intermediate risk volume to receive 60 Gy (CTV60) and low risk volume to receive 54 Gy (CTV54). The clinical target volume therefore included the primary disease, involved lymph nodes and potential areas of subclinical spread. For VMAT and PTV-based IMPT the CTVs were expanded with 5 mm to create corresponding PTVs. $CTV54_{ex}$/$PTV54_{ex}$ are the CTV54/PTV54 volumes without CTV60/PTV60 and CTV68/PTV68.

3.2.1 Volume delineation

Target volumes and organs at risk were delineated by a physician on the treatment planning CTs, a representative delineation of the CTVs and PTVs is shown in figure 3.1. In addition, volumes specific to IMPT-planning were made. The CTVs, parotid glands and medulla were transferred from the original CT to the re-CT using deformable registration. The volumes were evaluated and adjusted (if needed) by the responsible physician.

3.2.2 Plan optimization

Two IMPT plans were made for each patient, one based on PTV (IMPT-PTV) and one with robust optimization (IMPT-Robust). Based on literature it was decided to use two oblique anterior beams (50° and 310°) and one posterior beam (180°), see figure 3.2, similar to what is used at MD Andersson (27).

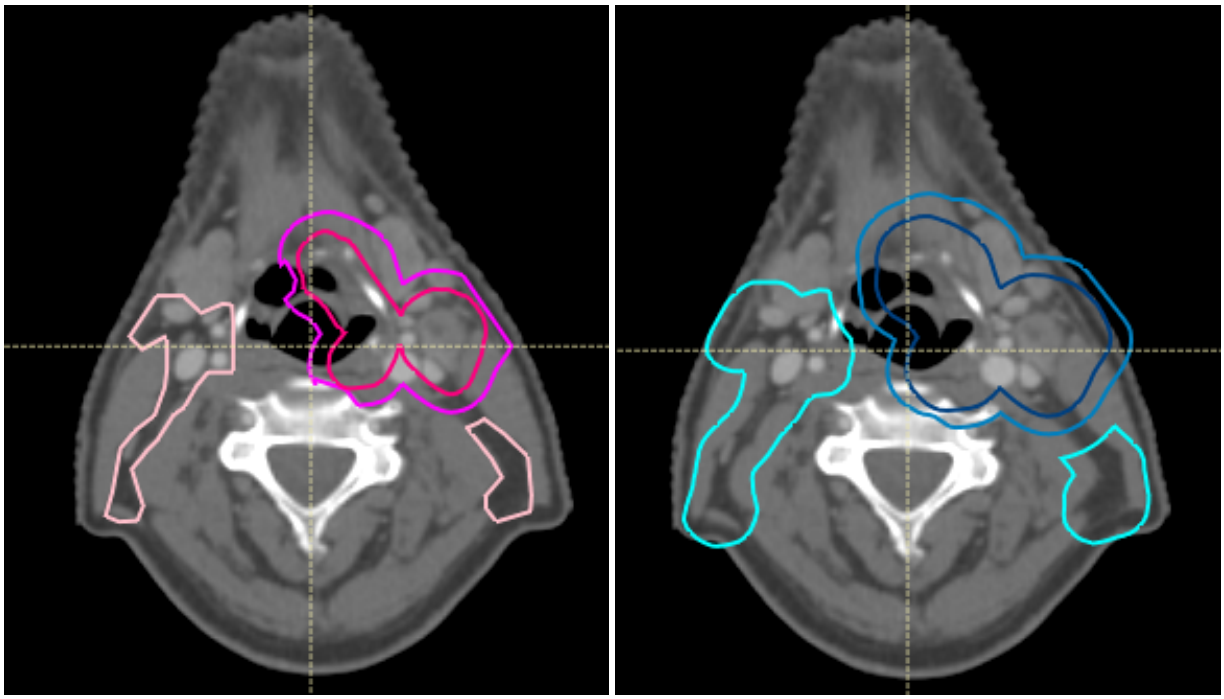

(a) (b)

Figure 3.1: Target volume delineation for patient 21 of (a) CTVs and (b) PTVs. Pale pink: $CTV54_{ex}$, Magenta: CTV60, Pink: CTV68, Bright blue: $PTV54_{ex}$, Blue: PTV60, Dark blue: PTV68.

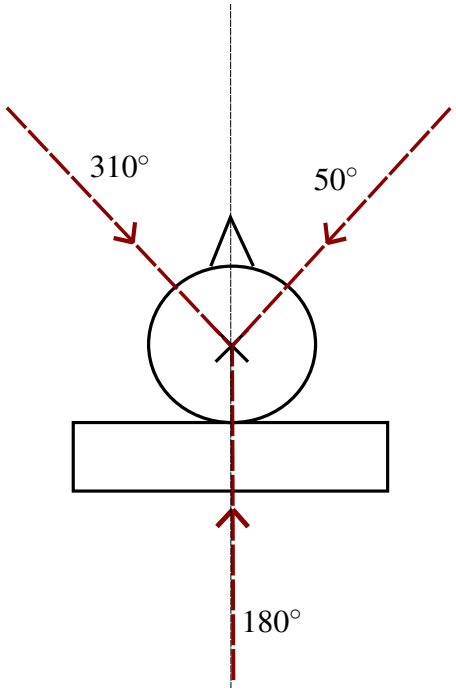

Figure 3.2: Field angles for IMPT for head and neck cancer.

The optimization objectives are shown in table 3.2. The minimum dose objectives for the different CTVs were given the highest weight because the CTV coverage has precedence over the rest of the objectives. The initial parotid dose objective was determined from the original VMAT plan, and then reduced as much as possible without compromising the target coverage.

Table 3.2: Optimization objectives used for IMPT.

ROI	Objective	Robust-function
CTV68	Uniform dose	Yes
CTV68	Minimum dose	Yes
CTV60	Minimum dose	Yes
$CTV54_{ex}$	Minimum dose	Yes
$CTV54_{ex}$	Uniform dose	Yes
Parotid	Max EUD	No
Medulla	Max dose	Yes
External	Dose fall-off	No

For patients 1-13 a range shifter of 40 mm was applied to all of the beams. For patients 18-23 a range shifter of 75 mm was applied to the two anterior beams and 40 mm for the posterior beam. Furthermore for patients 18-23 the anterior beams were restricted to treat the same side as the elective node only, this was done with objectives with zero weight applied to the left or right side of PTV54. Patient 1 was a unilateral case and for that patient the contralateral beam was removed to avoid unnecessary irradiation of healthy tissue.

The objectives chosen for the IMPT-Robust plans are given in table 3.2, in addition to which objectives were optimized with the robust-function. The robustness settings were set to 5 mm spatial shift in 6 directions and $\pm 3\%$ density change.

To evaluate the plans in a fast and easy manner, clinical goals were specified and utilized as a first impression on the quality of the treatment plan. Isodoses, DVHs and dose statistics were studied for further evaluation of the plans. If the plan was not deemed adequate modification of the objectives and further iterations had to be done. To be acceptable the IMPT plans were required to have a comparable target dose coverage as VMAT and the comparison was then done based on dose characteristics to the organs at risk.

3.3 NTCP

It was of interest to evaluate not only the dose change to the parotid glands between VMAT and IMPT but also if the probability of normal tissue complication was decreased for IMPT.

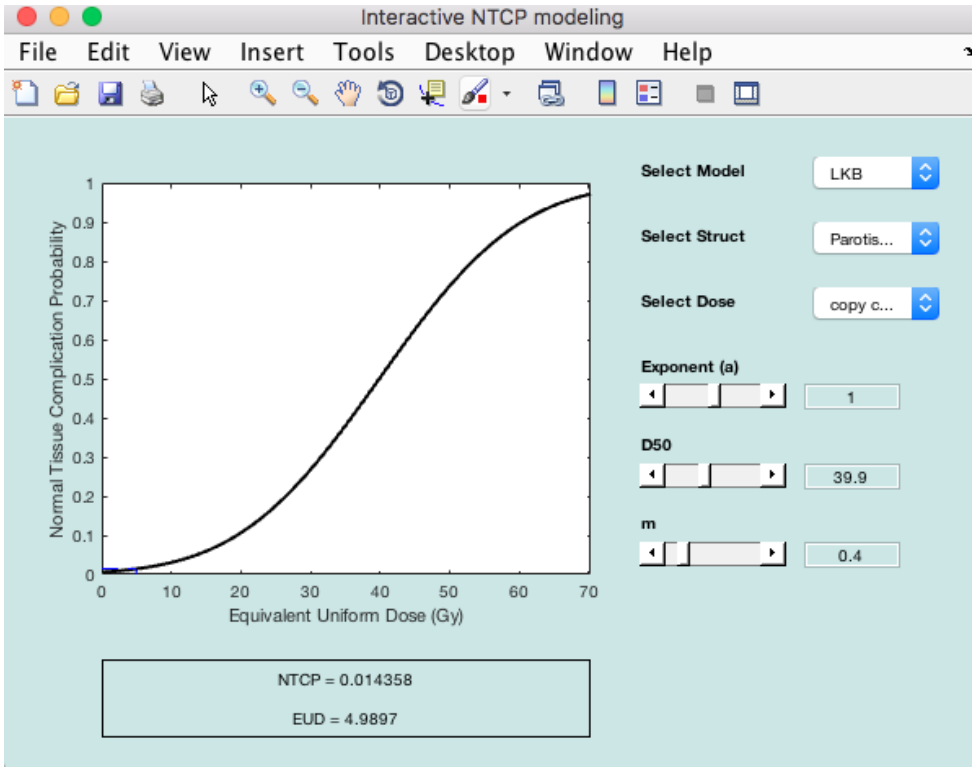

Figure 3.3: Picture from CERR showing the window for NTCP modeling.

NTCP values for parotid glands were calculated using the MATLAB (The Mathworks, Inc.) based program CERR (Computational Environment for Radiotherapy Research) (46). CERR calculates NTCP values from imported DVHs. A choice of NTCP models is offered as well as the possibility to change the parameters of the model. A snapshot of the window for NTCP modeling is shown in figure 3.3. In this thesis the LKB model was chosen with parameters n = 1, m = 0.4 and TD50 = 39.9, based on values for the parotid gland presented by Houweling et al. (47). To define a complication the threshold in this study was set to 25% of original saliva flow one year after the radiation treatment.

3.4 Plan evaluation

The main focus was the dose coverage to CTV, the mean dose to parotid glands and the maximum dose to medulla. D_{98} was chosen for evaluation of the target coverage, D_2 was also

extracted for the target volumes for comparison with VMAT. For VMAT and IMPT-PTV, V_{95} and V_{105} was also evaluated. The homogeneity index, equation 2.14, was calculated using x = 95%, while the conformity index, equation 2.15, was calculated using the 90% isodose.

3.4.1 Robust evaluation - perturbed treatment plans

Robust evaluation was done for 2 patients. The isocenter was shifted by 5 mm in 6 directions and the treatment plan was recalculated. Dose statistics on the CTVs and parotid glands were extracted.

3.4.2 Statistical analyses

To test for statistical significance a Student's t-test was used. The MATLAB function ttest(x,y) uses the paired-sample t-test and returns a test decision for the null hypothesis that the data in x and y comes from a normal distribution with mean equal to zero and unknown variance. The default setting is a 0.05 significance level (48). The t-test was used for both mean dose and NTCP of parotid glands, maximum dose to medulla and target volume coverage - checking for statistical significance in the difference between VMAT and IMPT and also between the original CT and re-CT for IMPT plans.

Box plots were made using MATLAB, where the red line are the median value (q_2). The edges of the box is the 25th percentile (q_1) and the 75th percentile (q_3). The outliers are shown in red plus-signs and a data point is defined as an outlier if it is larger than $q_3 + w(q_3 - q_1)$ or smaller than $q_3 - w(q_3 - q_1)$. w is the maximum whisker length and is set by default to 1.5. (48) The black crosses are the mean values.

3.5 Recalculating on new CT

In the original project a new CT was taken after 18 fractions and recalculated treatment plans were made for VMAT. In the present study the second CT was used to recalculate the original IMPT treatment plans to see if the plans are robust against uncertainties related to patient anatomy. Relevant dose statistics (CTV coverage and mean dose to parotid glands) were extracted and compared to the original CT for both IMPT-PTV and IMPT-Robust.

Chapter 4

Results

4.1 Dose distribution - target volumes

In figure 4.1 a snapshot from RayStation showing the dose distribution for a representative patient of this project work. The volumes of interest for target coverage is $CTV54_{ex}$, CTV60 and CTV68 for all plans, and PTV_{ex}, PTV60 and PTV68 for VMAT and IMPT-PTV. From figure 4.1 it is seen that all treatment techniques give conformal dose distributions and cover the target volumes. Also seen is the low-dose bath that is associated with VMAT, which is one of the reasons for investigating IMPT for therapy.

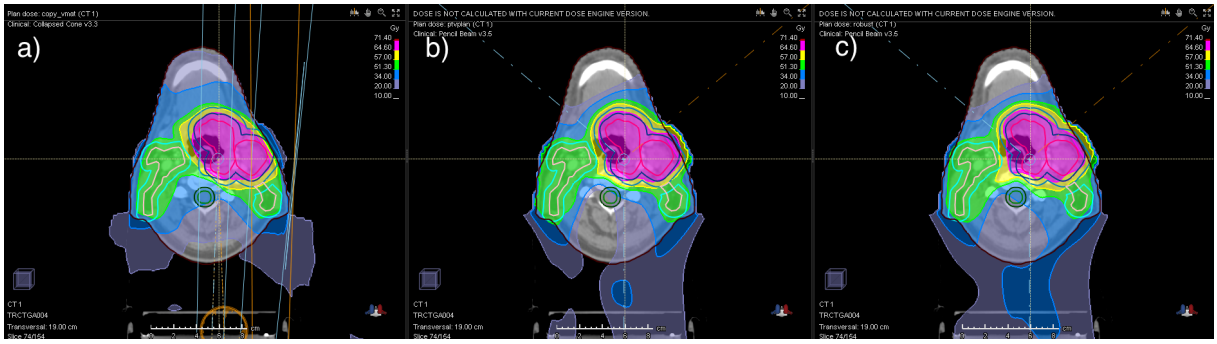

Figure 4.1: Example of dose distribution (patient 21) for a) VMAT b) IMPT-PTV c) IMPT-Robust taken from a representative patient. Pink: 64.6 Gy, Yellow: 57 Gy, Green: 51.3 Gy, Blue: 34 Gy.

4.1.1 54Gy volume

Dose distribution parameters for $CTV54_{ex}$ are shown in box plots in figure 4.2b and 4.2a. Mean D_{98} to $CTV54_{ex}$ was 53.1 Gy for VMAT, 52.8 Gy ($p = 0.006$) for IMPT-PTV and 52.5 Gy

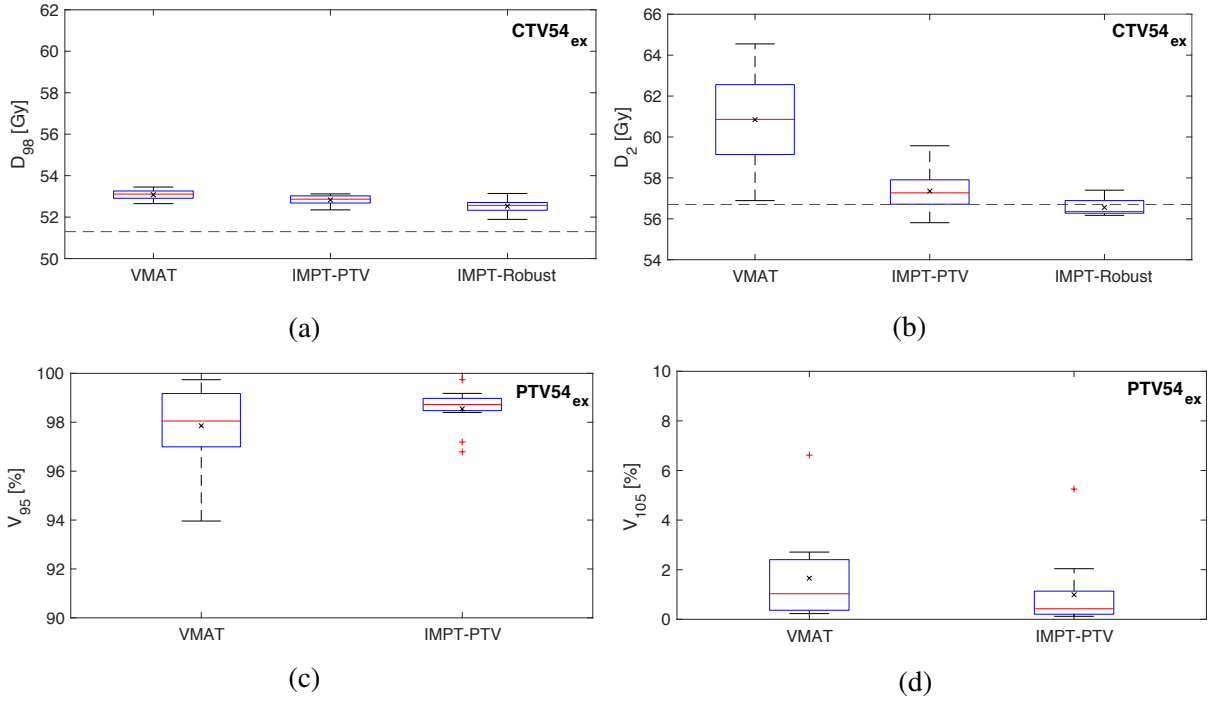

Figure 4.2: Dose/volume parameters of $CTV54_{ex}$/$PTV54_{ex}$ for all patients. (a) Dose given to at least 98% of $CTV54_{ex}$ [D_{98}]. (b) Dose given to the hottest 2% volume of $CTV54_{ex}$ [D_2]. (c) Volume receiving 95% of 54 Gy. [V_{95}]. (d) Volume receiving 105% of 54 Gy [V_{105}]. The dotted line indicates for (a) 95% and (b) 105% of 54 Gy.

($p = 0.002$) for IMPT-Robust. The p-values are calculated with a paired-sample t-test as described in section 3.4.2. For all patients, D_{98} to $CTV54_{ex}$ was $>$ 95% dose level (51.3 Gy), which is required for the target volume. D_2 was for all patients $>$ 105% dose level (56.7 Gy) for VMAT, whereas for IMPT 9 and 4 patients were $>$ 105% dose level for IMPT-PTV and IMPT-Robust, respectively.

In figure 4.2c the volume of $PTV54_{ex}$ receiving at least 95% of the prescribed dose is shown. The mean values of V_{95} for $PTV54_{ex}$ is 97.9% for VMAT and 98.6% ($p = 0.05$) for IMPT-PTV. For V_{105} (56.7 Gy), as shown in figure 4.2d, the mean value was 1.7% for VMAT, 0.99% for IMPT-PTV and 0.94% for IMPT-Robust. The largest volume receiving 105% of the prescribed dose for $PTV54_{ex}$ was 7% for VMAT and 5% for IMPT-PTV. Patient specific dose/volume parameters are given in appendix A.

4.1.2 60Gy volume

The dose distribution parameter, D_{98}, for CTV60 is shown in figure 4.3a. All patients plans were $>$ 95% dose level. In figure 4.3b the volume of PTV60 receiving at least 95% of 60 Gy

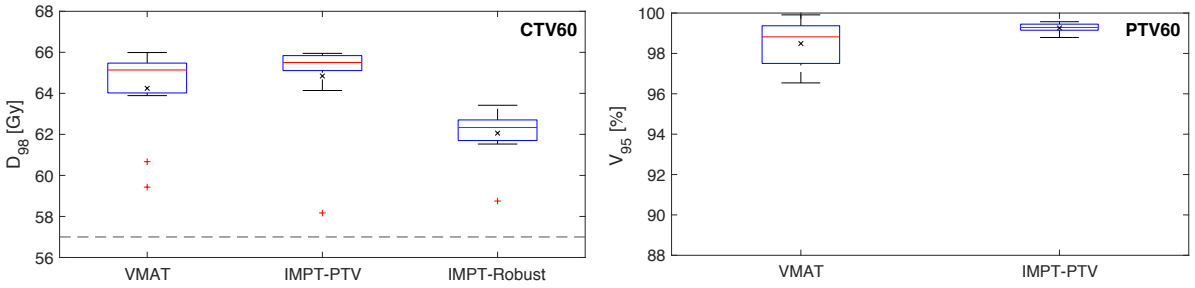

(a) IMPT-PTV (b) IMPT-Robust

Figure 4.3: Dose/volume parameters of CTV60/PTV60 for all patients. (a) Dose given to at least 98% of CTV60 [D_{98}]. (b) Volume receiving 95% [V_{95}] of 60 Gy. The dotted line indicates 95% of 60 Gy.

is given. The mean values of V_{95} for PTV60 was 98.5% for VMAT and 99.26% ($p = 0.04$) for IMPT-PTV. More detailed data is given in appendix A.

4.1.3 68Gy volume

For CTV68 the mean values of D_{98} are 67.1 Gy, 66.9 Gy ($p < 0.01$) and 66.1 Gy ($p = 0.3$) for VMAT, IMPT-PTV and IMPT-Robust, respectively. The distribution for D_{98} is seen in figure 4.4a. Figure 4.4b shows the maximum dose, D_2, for CTV68 and all patient plans were below the recommended 105% of 68 Gy, as seen by the dotted line.

The volume receiving 95% of the prescribed dose is shown in figure 4.4c. The mean values of V_{95} for PTV68 was 98.1% for VMAT and 99.4% ($p = 0.02$) for IMPT-PTV. V_{105}, shown in figure 4.4d, was small for both VMAT and IMPT-PTV, the largest volume receiving 105% of 68 Gy was 0.7%. Patient specific data is given in appendix A.

4.1.4 Homogeneity Index

The distribution of the homogeneity indices (HIs) are shown in figure 4.5a and 4.5b, for $CTV54_{ex}$ and CTV68, respectively. The HI for $CTV54_{ex}$ was on average better for IMPT plans than for VMAT, with values of 0.95 for both IMPT plans and a value of 0.91 for VMAT. For CTV68 the mean HIs were 0.97 for VMAT, 0.96 for IMPT-PTV and 0.95 for IMPT-Robust.

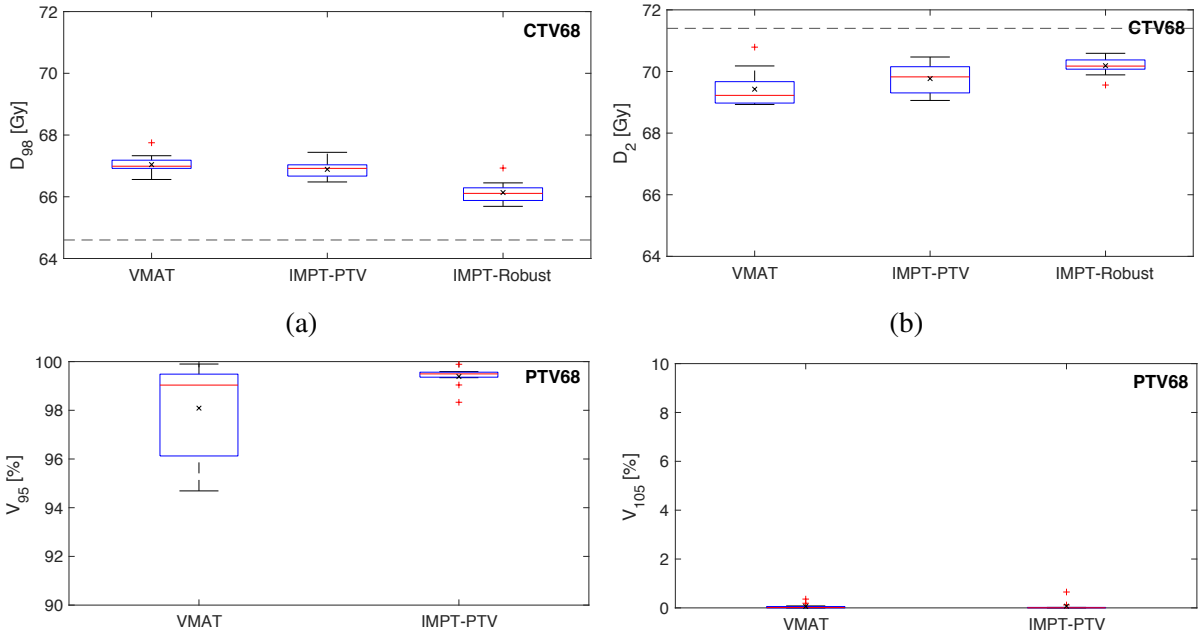

Figure 4.4: Dose/volume parameters of CTV68/PTV68 for all patients. (a) Dose given to at least 98% of CTV68 [D_{98}]. (b) Dose given to the hottest 2% volume of CTV68 [D_2]. (c) Volume receiving 95% of 68 Gy. [V_{95}]. (d) Volume receiving 105% of 68 Gy [V_{105}]. The dotted line indicates for (a) 95% and (b) 105% of 68 Gy.

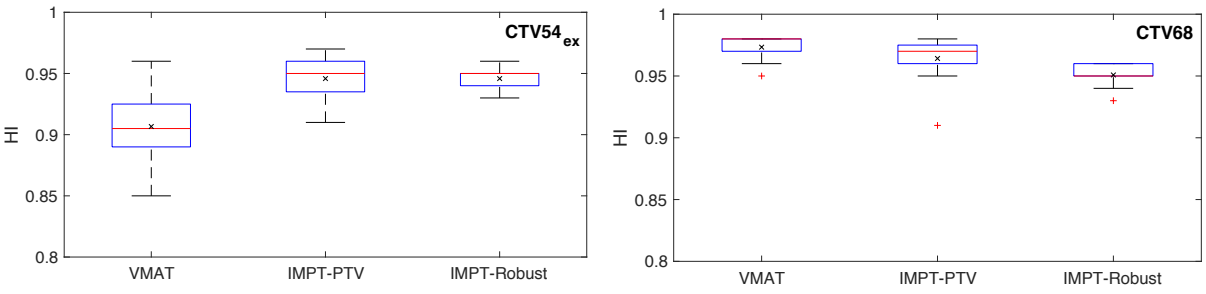

Figure 4.5: Homogeneity Index (HI) for VMAT, IMPT-PTV and IMPT-Robust plans.

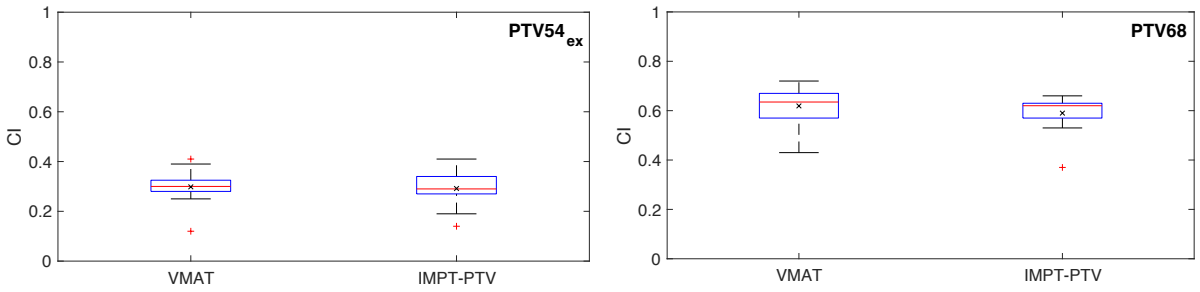

(a) CI for $PTV54_{ex}$ (b) CI for PTV68

Figure 4.6: Conformity Index (CI) for VMAT and IMPT-PTV plans.

4.1.5 Conformity Index

The distribution of the conformity indices (CIs) are shown in figure 4.6a for $PTV54_{ex}$ and 4.6b for PTV68. The mean values were similar for VMAT and IMPT-PTV: 0.3 for $PTV54_{ex}$ and 0.6 for PTV68.

4.2 Organs at risk

4.2.1 Parotid glands

The distribution of mean dose for each patients parotid glands is given in figures 4.7a and 4.7b. The average mean dose to the right parotid gland was 26.8 Gy for the VMAT plans. Both IMPT-plans reduced the mean dose to the right parotid gland compared to VMAT. The IMPT-PTV plan had an average mean dose of 23.6 Gy and the mean was 21.0 Gy for the IMPT-Robust plan: both dose reductions were statistically significant with a p-value of 0.04 and 0.002, receptively. For the left parotid gland the IMPT-plans led to decreased mean doses for all patients, with a mean of 33.9 Gy for VMAT and 28.3 Gy ($p = 0.001$) and 25.8 Gy ($p < 0.001$) for IMPT-PTV and IMPT-Robust, respectively. IMPT-PTV achieved lower mean dose than VMAT for 20 of 24 parotid glands, while IMPT-Robust had 22 parotid glands with lower mean dose than VMAT.

NTCP

NTCP for xerostomia was calculated for each parotid gland for all patient plans. The results are shown in figures 4.7c and 4.7d. The mean values for the right parotid gland were 23.7% for VMAT, 18.5% ($p = 0.08$) for IMPT-PTV and 14% ($p = 0.02$) for IMPT-Robust. The reduction of the mean NTCP values were therefore statistically significant for IMPT-Robust but not for IMPT-PTV. The reduction of the mean NTCP values were significant for both IMPT plans for

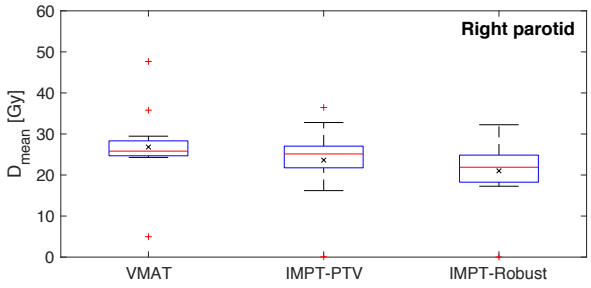

(a) Mean dose to the right parotid gland

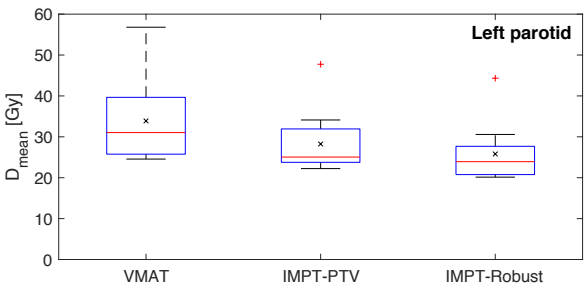

(b) Mean dose to the left parotid gland

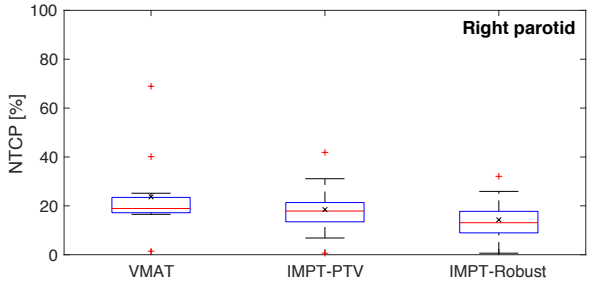

(c) NTCP for right parotid gland.

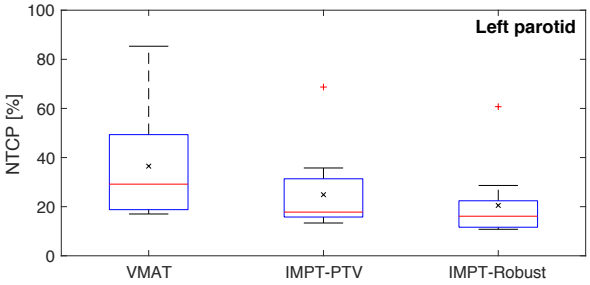

(d) NTCP for left parotid gland.

Figure 4.7: Mean dose and NTCP for parotid glands. The dotted line indicates the recommended mean dose threshold, 26 Gy, for parotid glands.

the left parotid. The mean values for VMAT, IMPT-PTV and IMPT-Robust were 36.5%, 24.9% ($p = 0.002$) and 20.5% ($p < 0.001$). 9 of 12 patients had a substantial decrease in NTCP values ($> 10\%$) for either IMPT-PTV or IMPT-Robust, for specific data see table B.2 in appendix B. A total of 8 patients had decreased values for both IMPT-PTV and IMPT-Robust, and of these 7 patients had lowest NTCP-values with IMPT-Robust.

4.2.2 Medulla

The maximum dose to a 0.1 cm^3 of the medulla is shown in figure 4.8a. The mean value for VMAT is 41.5 Gy while the IMPT plans resulted in mean values of 38.7 Gy for IMPT-PTV and 37.0 Gy for IMPT-Robust. Only the decrease for IMPT-Robust was statistically significant with a p-value of 0.04. All maximum doses for medulla are below the recommended 45 Gy, except for one patient, who got 48.4 Gy in the original VMAT plan. For more detailed data see table B.3 in appendix B.

A PRV-margin for medulla of 3 mm was used here. The maximum doses are given in figure 4.8b. All patients, except for one patient for VMAT and 2 patients for IMPT-PTV, are below

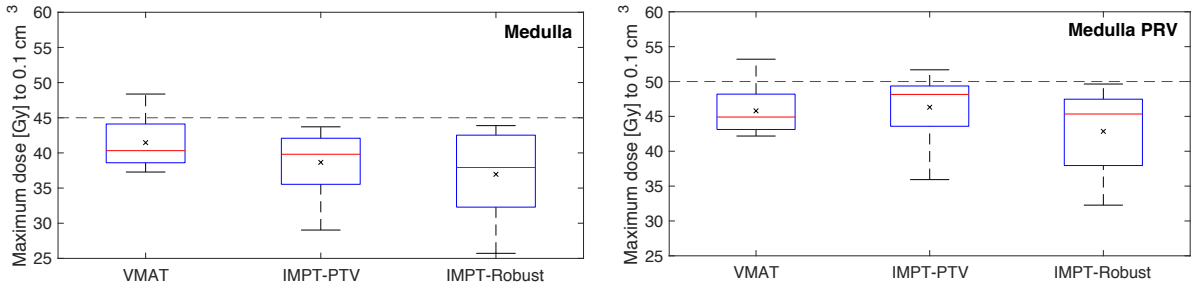

(a) (b)

Figure 4.8: Maximum dose to 0.1 cm^3 for (a) medulla and (b) medulla with a 3 mm margin = medulla PRV. The dotted line indicates the recommended maximum dose threshold, (a) 45 Gy for medulla and (b) 50 Gy for medulla PRV.

the recommended maximum dose of 50 Gy.

4.2.3 Irradiated volume

The mean irradiated volume of the patient bodies are shown in figure 4.9. The bar plot shows that VMAT results in a larger "low dose bath" than IMPT plans. The volume irradiated with high doses ($>$ 40 Gy) are similar across the modalities. In figure 4.10 the absolute volumes receiving $>$ 95% of the prescribed doses for $CTV54_{ex}$, CTV60 and CTV68 for IMPT-PTV and IMPT-Robust is given.

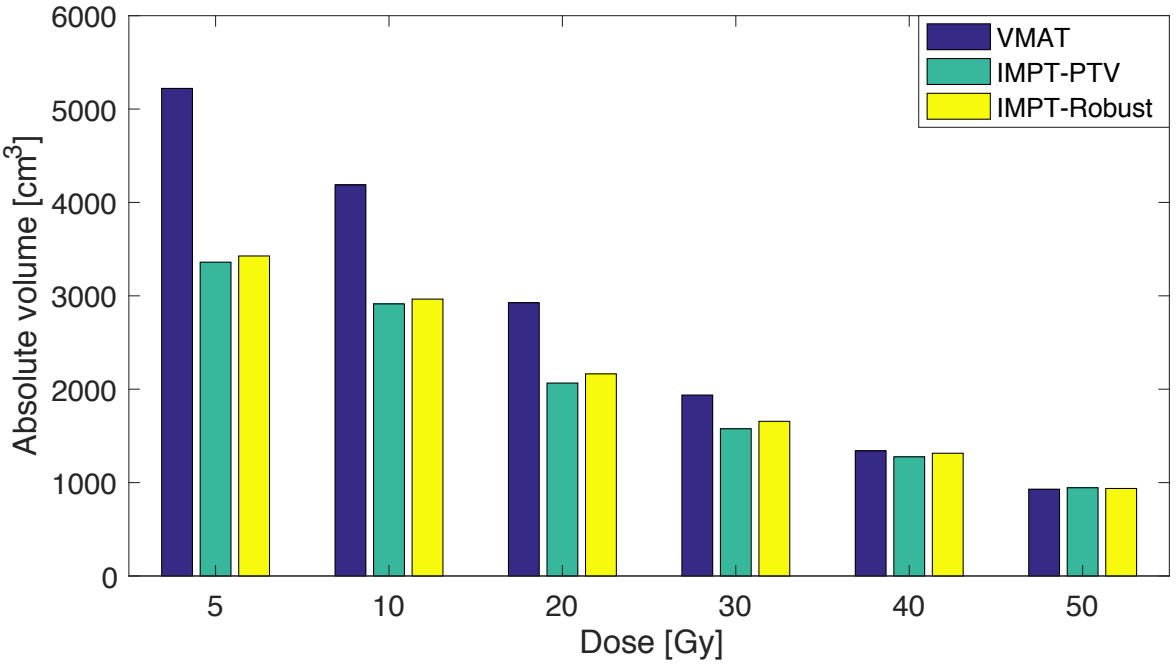

Figure 4.9: Absolute volume [cm^3] of the body irradiated to at least 5 Gy, 10 Gy, 20 Gy, 30 Gy, 40 Gy and 50 Gy. The volumes were averaged over the 12 patients included in the study.

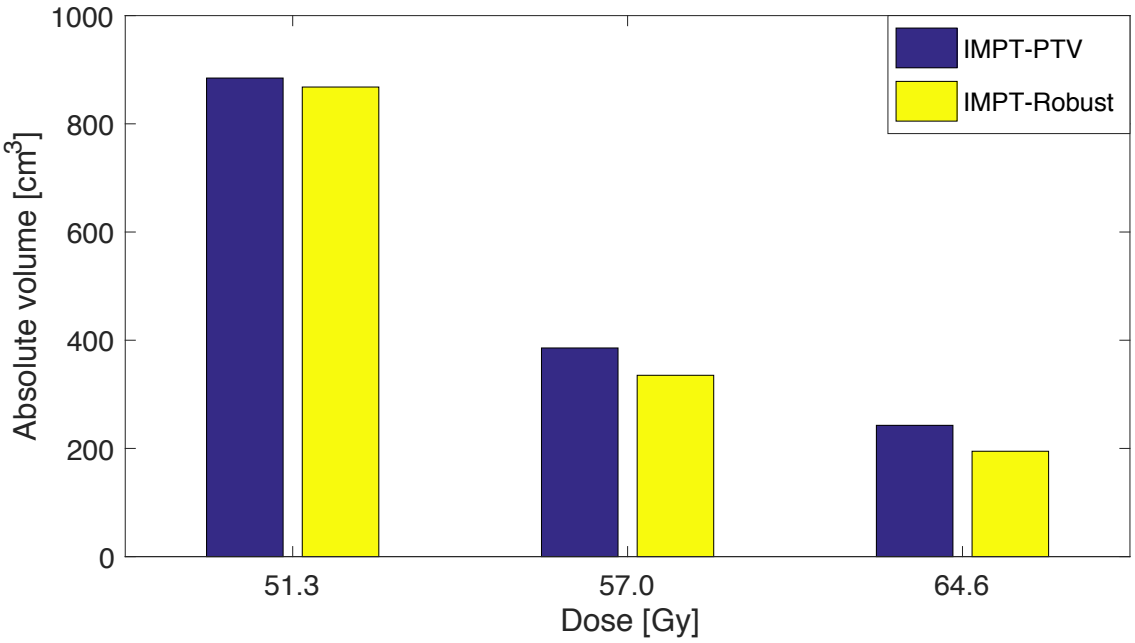

Figure 4.10: Absolute volume [cm^3] of the body irradiated to at least 51.3 Gy, 57.0 Gy and 64.6 Gy. The volumes were averaged over the 12 patients included in the study.

4.3 Re-CT

The repeat CT (CT2) was taken after 18 fractions (36 Gy) for all patients and the treatment plans were re-calculated. Minimum dose (D_{98}) for the target volumes are given in tables 4.1, 4.2 and 4.3. The dose difference between CT2 and CT1 is also included there (CT2 - CT1) . It can be seen from these tables that the majority of the treatment plans got lower minimum doses to the CTVs on CT2 compared to CT1. Patient 1 is the only case with unilateral cancer, and also had a substantial increase in the $CTV54_{ex}$ volume for CT2 (CT1 = 77 cm^3 vs CT2 = 91 cm^3).

4.3.1 Target coverage - CTV

CTV54

Table 4.1 gives the difference CT2 - CT1 and shows that for most patients the minimum dose was lower in CT2 than CT1. The minimum dose should not be below 51.3 Gy for $CTV54_{ex}$, and this was achieved for 6 of 12 patients for IMPT-PTV and for 11 patients for IMPT-Robust. The paired-sample t-test shows that the differences between CT2 and CT1 were not statistically significant with p-values of 0.06 for IMPT-PTV and 0.27 for IMPT-Robust.

Table 4.1: Minimum dose [Gy] (D_{98}) for $CTV54_{ex}$ calculated on the two CTs for each patient. Diff. is the difference CT2 - CT1. * indicates cases where the dose has dropped below the minimum dose limit of 51.3 Gy.

	IMPT-PTV			**IMPT-Robust**		
Patients	CT1 [Gy]	CT2 [Gy]	**Diff.** [Gy]	CT1 [Gy]	CT2 [Gy]	**Diff.** [Gy]
1	53.01	31.17*	-21.84	52.27	24.99*	-27.28
2	52.93	51.44	-1.49	52.62	52.33	-0.29
3	52.86	50.39*	-2.47	52.56	51.68	-0.88
4	53.12	50.84*	-2.28	51.89	51.77	-0.12
6	52.45	51.48	-0.97	52.57	51.79	-0.78
9	52.35	51.97	-0.38	52.40	52.27	-0.13
13	52.73	50.75*	-1.98	52.27	52.43	0.16
18	52.83	51.80	-1.03	52.59	52.12	-0.47
19	52.87	49.66*	-3.21	53.14	52.72	-0.42
20	53.04	52.31	-0.73	52.39	52.65	0.26
21	53.12	52.55	-0.57	52.79	52.56	-0.23
23	52.63	46.82*	-5.81	52.84	51.55	-1.29
p-value			0.06			0.27

CTV60

For the CTV60 the minimum dose should not be below 57 Gy. As given in table 4.2, only one case for IMPT-Robust had a dose below this threshold. Only the IMPT-PTV difference between CT2 and CT1 was significant with $p = 0.01$.

Table 4.2: Minimum dose [Gy] (D_{98}) for CTV60 calculated on the two CTs for each patient. Diff. is the difference CT2 - CT1. * indicates cases where the dose has dropped below the minimum dose limit of 57 Gy.

	IMPT-PTV			**IMPT-Robust**		
Patients	CT1 [Gy]	CT2 [Gy]	**Diff.** [Gy]	CT1 [Gy]	CT2 [Gy]	**Diff.** [Gy]
1	65.92	57.55	-8.37	62.37	56.16*	-6.21
2	64.95	62.29	-2.66	62.30	60.24	-2.06
3	65.46	65.03	-0.43	61.53	61.67	0.14
4	65.60	64.13	-1.47	61.64	61.00	-0.64
6	65.76	64.45	-1.31	62.72	63.36	0.64
9	58.17	58.29	0.12	58.75	59.27	0.52
13	64.14	62.50	-1.64	61.76	60.49	-1.27
18	65.55	64.17	-1.38	62.29	61.25	-1.04
19	65.27	63.65	-1.62	62.69	62.61	-0.08
20	65.95	65.76	-0.19	62.75	62.57	-0.18
21	65.43	64.63	-0.80	63.42	63.39	-0.03
23	65.95	61.26	-4.69	62.51	60.52	-1.99
p-value			0.01			0.09

CTV68

For CTV68 the minimum dose should not be below 64.6 Gy. As shown in table 4.3, 3 patients had a value below 64.6 Gy for IMPT-PTV, while 2 patients had the same for IMPT-Robust. Both IMPT-PTV and IMPT-Robust were statistically significant with p-values 0.01 and 0.04, respectively.

Table 4.3: Minimum dose [Gy] (D_{98}) for CTV68 calculated on the two CTs for each patient. Diff. is the difference CT2 - CT1. * indicates cases where the dose has dropped below the minimum dose limit of 64.6 Gy.

	IMPT-PTV			**IMPT-Robust**		
Patients	CT1 [Gy]	CT2 [Gy]	**Diff.** [Gy]	CT1 [Gy]	CT2 [Gy]	**Diff.** [Gy]
1	67.44	62.66*	-4.78	65.69	63.61*	-2.08
2	66.94	66.11	-0.83	65.83	65.47	-0.36
3	67.10	66.82	-0.28	65.79	65.78	-0.01
4	66.48	65.05	-1.43	66.25	65.86	-0.39
6	66.91	66.49	-0.42	66.18	66.16	-0.02
9	66.50	66.17	-0.33	65.93	65.58	-0.35
13	66.93	66.04	-0.89	65.98	65.91	-0.07
18	66.97	65.50	-1.47	66.04	65.67	-0.37
19	66.64	64.13*	-2.51	66.93	66.51	-0.42
20	67.26	66.50	-0.76	66.29	66.08	-0.21
21	66.79	66.46	-0.33	66.45	66.65	0.20
23	66.70	62.67*	-4.03	66.29	64.40*	-1.89
p-value			0.01			0.04

4.3.2 Parotid Glands

In figure 4.11, the mean dose to the parotid glands as calculated in CT1 and CT2 are shown. The average change (between CT2 and CT1) in the mean dose for the right parotid was 1.79 Gy (IMPT-PTV) and 1.07 Gy (IMPT-Robust). For the left parotid gland IMPT-PTV had a mean difference of 0.5 Gy, and IMPT-Robust of 0.09 Gy. The mean dose difference, for the individual patients, between CT2 and CT1 ranged from -7.3 Gy to 3.4 Gy.

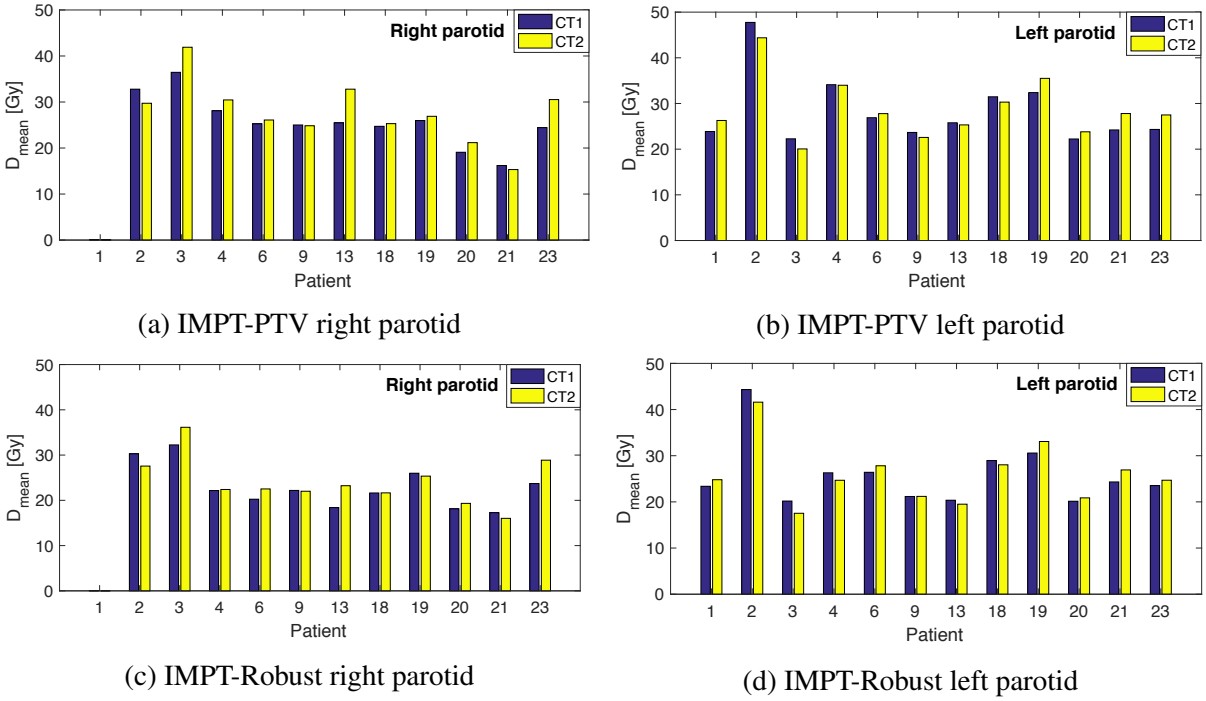

(a) IMPT-PTV right parotid

(b) IMPT-PTV left parotid

(c) IMPT-Robust right parotid

(d) IMPT-Robust left parotid

Figure 4.11: Mean dose for parotid glands for CT1 and CT2.

4.3.3 Medulla

The maximum dose to the medulla for CT1 and CT2 can be seen in figure 4.12a and 4.12b for all patients. The maximum dose to the medulla was above the recommended 50 Gy for 1 patient for IMPT-PTV, and none for IMPT-Robust. Of the 12 patients, 8 patients had an increase in maximum dose to the medulla for IMPT-PTV and IMPT-Robust. The maximum dose difference to the medulla, for each patient, between CT2 and CT1 ranged from -7.0 Gy to 7.8 Gy.

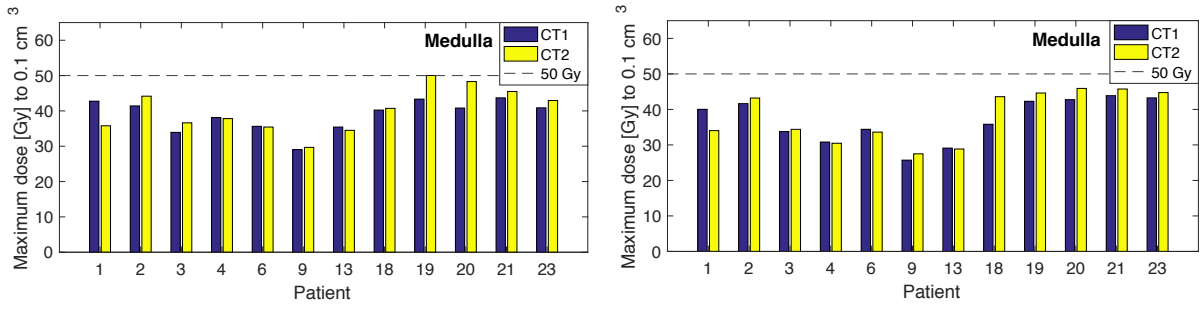

(a) IMPT-PTV

(b) IMPT-Robust

Figure 4.12: Maximum dose to 0.1 cm^3 for medulla calculated in CT1 and CT2. The dotted line indicates the recommended maximum dose threshold, 50 Gy, for medulla.

4.4 Perturbed treatment plans

To check the robustness of the IMPT treatment plans, 2 representative patients were chosen and their treatment plans perturbed by shifting the isocentre by 0.5 cm in 6 directions. The resulting change in dose coverage to target volumes ($CTV54_{ex}$ and CTV68) and mean doses to both parotid glands are given in figure 4.13 for patient 06. From this it can be seen that the greatest differences is for the parotid gland, but that the change cancels for the different directions, e.g. a shift to the right gives a change similar but opposite of a shift to the left. The bar plot shows that the change in dose for the target coverage in IMPT-Robust is less than for IMPT-PTV. This is supported by figure 4.14, which illustrates similar data for patient 21. For more detailed data, see appendix C.

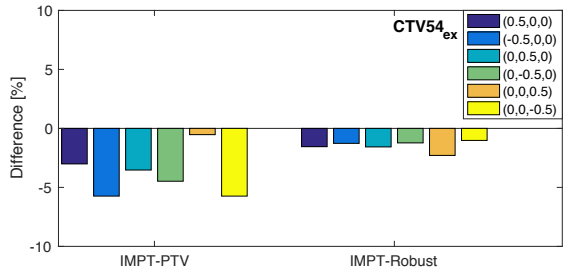

(a) $CTV54_{ex}$ D_{98}

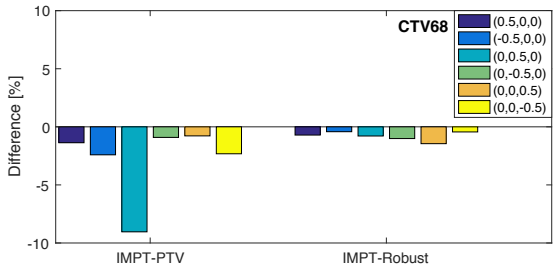

(b) CTV68 D_{98}

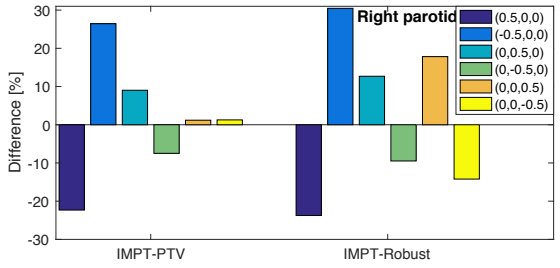

(c) Right parotid D_{mean}

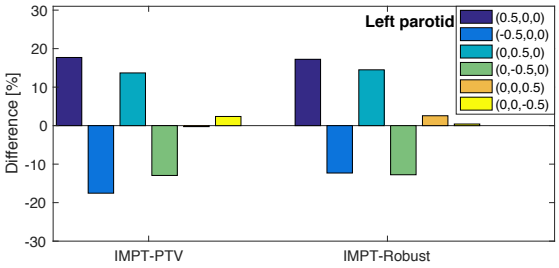

(d) Left parotid D_{mean}

Figure 4.13: Relative difference in doses between non-perturbed and perturbed treatment plans for patient 06. The colored bars correspond to a shift in direction (x,y,z) and is given i cm. A negative sign indicates a dose reduction, while a positive sign is a dose increase.

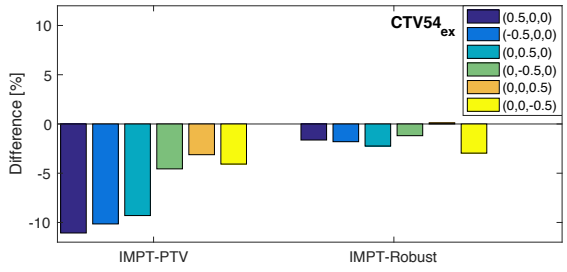

(a) $CTV54_{ex}$ D_{98}

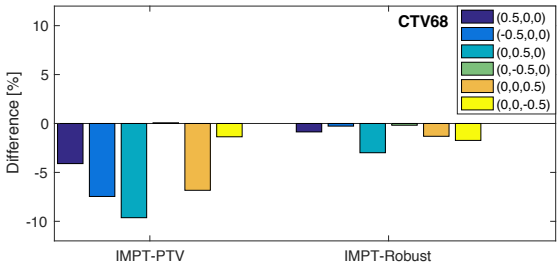

(b) CTV68 D_{98}

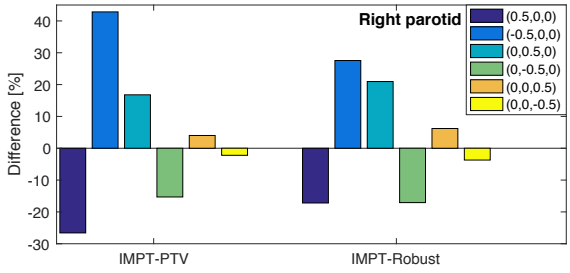

(c) Right parotid D_{mean}

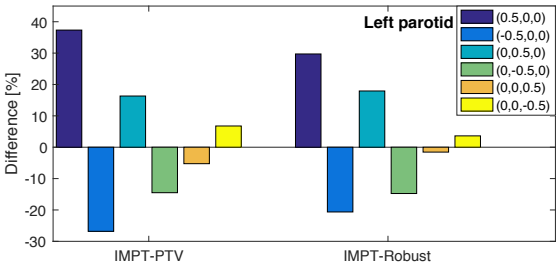

(d) Left parotid D_{mean}

Figure 4.14: Relative difference in doses between non-perturbed and perturbed treatment plans for patient 21. The colored bars correspond to a shift in direction (x,y,z) and is given i cm. A negative sign indicates a dose reduction, while a positive sign is a dose increase.

Chapter 5

Discussion

5.1 Target volumes - VMAT vs IMPT

The main aim of this thesis was to evaluate the possible benefits of proton therapy for head and neck cancer. In order to do a fair comparison with VMAT plans, the target dose coverage was required to be equal (or better) than the VMAT plans. Figures 4.2 and 4.4 confirm that the target dose coverage for IMPT-PTV and IMPT-Robust plans were indeed comparable to that of the VMAT plans. For $CTV54_{ex}$ the median value for the maximum dose was highest for VMAT, while for CTV68 the median was highest for the IMPT-Robust plan. Because the dose gradient is steeper for protons, the higher doses do not ”leak” from CTV68/CTV60 to CTV54, as it might do for VMAT.

The mean doses to $CTV54_{ex}$ are comparable between the treatment plans, with VMAT having one outlier at 57 Gy and larger whiskers, indicating that the IMPT plans are more similar across patients than VMAT. For CTV68 the mean doses are even more alike, and the dose coverage is almost exactly the same with mean values of 68.2 Gy (VMAT), 68.1 Gy (IMPT-PTV) and 68.2 Gy (IMPT-Robust). These results are not surprising since the plans are made with the same prescribed dose and are required to have equal target dose coverage.

The homogeneity index (HI) is also similar, with a mean of 0.95 for the IMPT plans for $CTV54_{ex}$ versus 0.91 for VMAT. For CTV68 VMAT had the highest mean value with 0.97, but IMPT-Robust was only slightly lower with 0.95.

PTV-based evaluation was only done for VMAT and IMPT-PTV, since PTVs are not used for IMPT-Robust. Overall, the IMPT-PTV plans had less patient-to-patient variability than VMAT. Dose coverage of the PTVs were overall better with IMPT than VMAT. VMAT has larger whiskers (i.e. larger differences between minimum and maximum values) for V_{95}. The difference in V_{95} between VMAT and IMPT-PTV for both $PTV54_{ex}$ and PTV68 was statistically significant with p-values of 0.05 and 0.02, respectively. For V_{105}, both plans had outliers well above the median value, but all patients had volumes of less than 1% getting 105% of the prescribed dose.

The conformity index (CI) was compared for VMAT and IMPT-PTV and the differences were small and not significant. Previous work by van de Water et al. have reported a marked improvement in the CI for IMPT (49), but this was not found in the present study. A reason is that $PTV54_{ex}$ is a large volume with the high dose volumes excluded. PTV60 and PTV68 are pushed towards high dose levels, but these are not included in $PTV54_{ex}$, resulting in poorer CIs.

As expected, for IMPT plans the ”low-dose-bath” associated with VMAT is not an issue. The average volumes receiving $<$20 Gy is lowest for IMPT-PTV. But IMPT-Robust volumes are not significantly higher than IMPT-PTV, as shown in figure 4.9. From approximately 40 Gy the irradiated volumes are similar for VMAT and IMPT.

The volume irradiated to clinical dose levels are as shown in figure 4.10. It is somewhat surprising that IMPT-Robust has the smallest volumes irradiated because one would think that when set up and range uncertainties are taken into account, high doses has to be given outside the CTVs to ensure adequate target coverage. A reason may be that the robust optimization algorithm is more complex and takes into account more uncertainties than conventional margins, resulting in dose distributions that is more conformed around the CTVs.

5.2 Organs at risk - VMAT vs IMPT

5.2.1 Parotid glands

It was of interest to evaluate the potential for parotid dose sparing using IMPT. Figure 4.7 shows that the reduction of dose to the parotid glands were significant and that IMPT-Robust plans on

average gave the lowest mean parotid doses.

van de Water et al. reported that the reduction in mean dose to the parotid glands for IMPT compared to IMRT varied widely among patients (49). This was also seen in the present study as not all patients had a large decrease in mean parotid dose, and two patients even had an increase in dose with IMPT (PTV-based and robust optimized) compared to VMAT. van de Water et al. further discussed that reporting only population based differences between two modalities may not be sufficient to investigate the potential benefits of one technique over another (49). The authors came to the conclusion that the best way probably is to look at each individual patient and compare the different techniques, before selecting who benefits from one technique over another.

In the present study, 11 of the 12 included patients had bilateral oropharynx cancer. The last one had unilateral oropharynx cancer. This one patient (patient 1) has results that are not consistent with the rest. The contralateral (the right) parotid gland received minimal dose for IMPT. For VMAT the mean dose was 5 Gy. Stormberger et al. concluded from their study that IMPT could potentially reduce the risk of xerostomia for unilateral cases (50).

5.2.2 The use of NTCP

NTCP was calculated to see if a statistically significant reduction in parotid dose also translates into a clinically significant difference. Xerostomia is a common side effect after irradiation to the head and neck area, and was therefore chosen as an endpoint for the NTCP calculations (51). The highest NTCP was found for the same patient: 85.32% for VMAT, 68.71% for IMPT-PTV and 60.71% for IMPT-Robust. The results are supported by Jakobi et al. (52), who found that IMPT led to lower NTCP values than IMRT. van Djik et al. compared NTCP values for IMRT and robust optimized IMPT and got a reduction of on average 17% for xerostomia (35).

The use of NTCP to predict the effectiveness of dose reduction to organs at risk is dependent on the choice of model, model parameters and the patient group. Several models exist, both analytical and empirical, that will yield slightly different NTCP values. In this thesis the LKB model was chosen, based on the fact it is commonly used and because the mean dose model (LKB with n = 1) is documented to be the best at describing the dose-response relationship for

the parotid gland (Houweling et al. (47)).

The LKB model use DVH information to calculate the NTCP. DVHs do not give spatial information, such as the location of a high- or low-dose area. Konings found region-dependent volume effects for the parotid glands in rats (53), and this suggests that DVHs may be an inadequate method for NTCP-calculations. Houweling et al. propose that a three-dimensional dose distribution based NTCP-model can describe the dose response of the parotid gland more appropriately (47).

Protons have a spatial dose distribution that is different from photons because of the fundamental difference in their interactions with tissue. This was pointed out by van de Water et al., and the validity of using NTCP model parameters obtained from photon radiation therapy was questioned (49). The Houweling et al. study (47) used data from patients treated with conventional radiation therapy and IMRT and it is possible that this to some extent may have led to unfair comparison of VMAT and IMPT in this thesis. The calculated NTCP values should therefore be regarded as an indication of clinical burden rather than the actual probability of complication.

5.2.3 Medulla

Medulla is a serial organ and the main concern is the maximum dose. A high dose to a small volume may result in functional impairment, and a threshold dose of 45 Gy is commonly applied. Based on our results, IMPT managed to keep the dose below the threshold for all patients, whereas VMAT was above for one patient. Overall, the mean values indicate that it is easier to spare the medulla when using IMPT. This is as expected, as protons have a certain range, and deposit no dose behind the Bragg peak. However, the uncertainties that influence the exact range of protons can lead to higher doses to the medulla.

The main point of including the medulla as an organ at risk is to ensure that the maximum dose does not exceed the tolerance level. The benefit of IMPT is not evident here, as VMAT manages to do this as well. However, the results indicate that it may be easier to reduce the dose to medulla using robust optimized IMPT rather than PTV-based or VMAT.

5.3 PTV-based IMPT vs robust optimized IMPT

For radiotherapy planning in general, the use of PTVs are a widespread and verified method to take into account setup errors associated with radiation therapy delivery. The margin between CTV and PTV is meant to ensure coverage of the CTV with a probability of at least 95% when uncertainties are included. The PTV method works for photons since the variations in dose is relatively small when faced with setup uncertainties. For proton therapy, the PTV concept is not always considered to be an adequate method because protons behave in a completely different way than photons (9; 54). Small uncertainties in set up or patient anatomy may introduce large perturbations in the dose distribution.

When making the robust optimized treatment plans it was hard to know what was good enough. PTV-based IMPT was easier to compare to VMAT, and it was also easier to know when the target coverage was adequate. With IMPT-Robust the dose distribution looked different from IMPT-PTV, often with less margin from the CTVs, and it was difficult to see how this could be robust. It was also challenging to know which weight to put on the different objectives used for treatment planning. There was a lot of trial and error, and the best method for robust optimization may not have been utilized.

5.3.1 Re-CT

The issue with PTV-based IMPT is addressed in this master thesis, by creating two different IMPT plans for each patient (PTV-based and robust optimized). These plans were then recalculated on a new CT (CT2) in order to evaluate the robustness of the dose to target volumes and organs at risk. The differences in dose between CT1 and CT2 was on average larger for IMPT-PTV than IMPT-Robust for all target volumes, and for all but one (left parotid gland) OAR (section 4.3). This is expected based on the literature because of increasing evidence that PTV is not sufficient to account for set up errors and patient anatomy changes (9; 11).

For patient with large differences in the delineated volumes in CT1 vs CT2, the dose distribution will not cover the target volumes in CT2; this was clearly seen for patient 1. Patient 1 had a somewhat larger $CTV54_{ex}$ in CT2 than in CT1 (91 cm^3 vs 77 cm^3). The $CTV54_{ex}$ was delineated on 1.6 cm beyond the original in CT2 and explains the great difference in D_{98} in

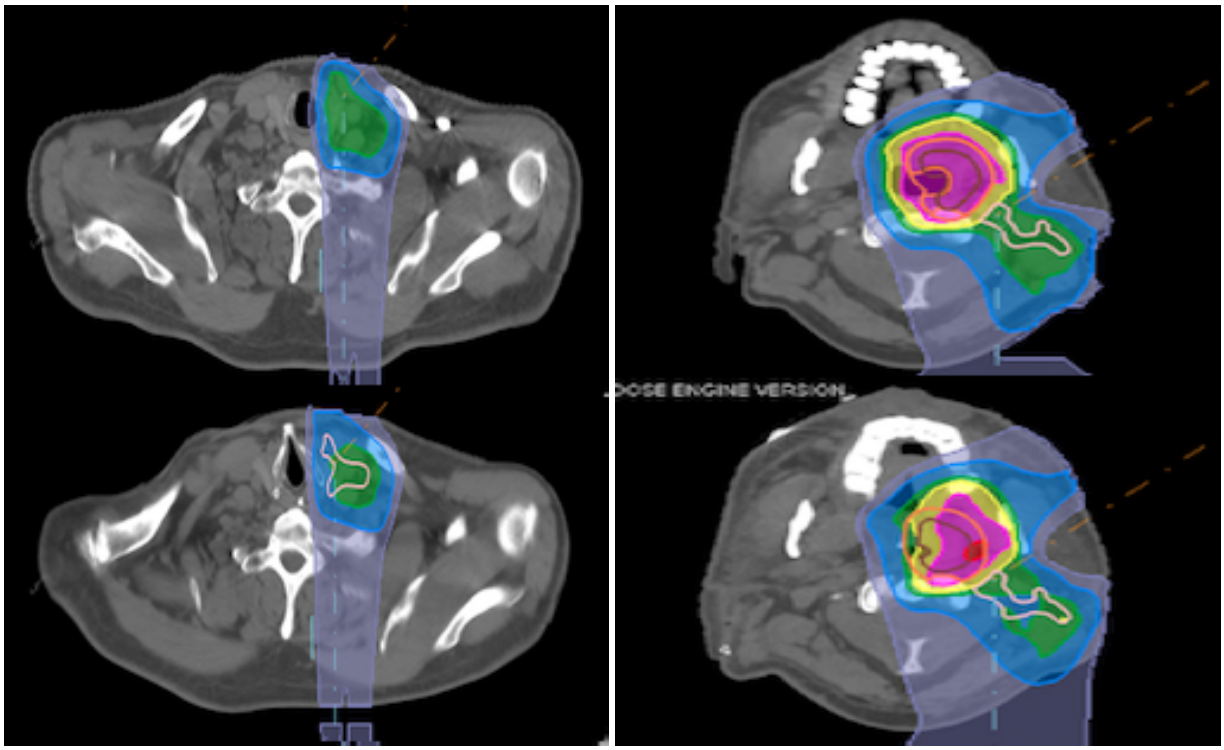

(a) Dose distribution lower slice (b) Dose distribution target volumes

Figure 5.1: Dose distributions from the unilateral case showing where the target volume coverage fails for the re-CT. Upper image is CT1 and lower is CT2.

CT2 and CT1, as seen in table 4.1. The reason for this difference is that the patient setup is slightly different in the two CTs. It was observed that the registration did not match as well in the lower parts of the CT scans, because the patient was placed somewhat differently on the table. In figure 5.1a the first slice where only CT2 has a $CTV54_{ex}$ is shown, and already in this slice the target coverage is poor. Figure 5.1b also shows a reason for the poor target coverage, all target volumes do not have adequate dose coverage in this slice. It is therefore possible that two beams are not enough to be robust against set up errors and three beams should be used on unilateral cases as well. Two beams were used for the unilateral case in the present study to minimize unnecessary dose to healthy tissue.

Table 4.1 shows that several of the cases were below the required minimum dose for $CTV54_{ex}$, and this result suggests a need for re-planning on the new CT. However, this was mostly seen for the PTV-based IMPT; the robust optimized IMPT was fairly robust against patient anatomy/setup changes, except for patient 1. Patient 1 also had a lower than optimal D_{98} for both CTV60 and CTV68 for CT2. The patients that had lower than 95% of the prescribed dose for CTV68 also got doses well below the minimum dose limit for $CTV54_{ex}$, and these patients

might therefore benefit the most from a re-planning during treatment if PTV-based IMPT is used.

Zhang et al. conducted a study to find the optimal time for new CTs for IMRT and found that a new CT (and re-planning) at week 1, 2 and 5 was optimal when considering mean dose to the parotid glands (55). The results in figure 4.11 show small differences between CT1 and CT2, but also between IMPT-PTV and IMPT-Robust, indicating that re-planning is not necessary when only the parotid glands are of concern. The exceptions are patient 3, 13 and 23, which had a fairly large increase (> 5 Gy) for one parotid gland in CT2 and therefore might actually have an advantage of re-planning.

The maximum dose to the medulla for the re-CT is of interest because of the seriality of the organ. If a dose above 50 Gy is given, there is a risk for functional impairment. It will not matter that the dose in CT1 is well below the threshold if the patients anatomy changes to such an extent that the medulla gets above the threshold dose at a later stage of the radiotherapy. From figure 4.12 it is seen that only 1 patient for IMPT-PTV have an increase in dose that accumulate to a too high dose for the medulla. This dose is just slightly above 50 Gy and should not have a great impact. For IMPT-Robust, the highest maximum dose was 46 Gy.

The literature on adaptive treatment planning of head and neck cancer focuses on photon therapy (55). However, there are some reports also in proton therapy. Kraan et al. found that adaptive treatment planning, with a new CT midway, positively affected the dose delivery to the target volumes for IMPT (8). Simone et al. found that adaptive treatment IMPT significantly reduced dose to several organs at risk (12). Because of the physical properties of protons it is to be expected that adaptive treatment planning will be at least as important for IMPT as for IMRT/VMAT.

5.3.2 Perturbed treatment plans

For 2 patients, the treatment plans were perturbed in 6 different directions, which resulted in a decrease in target coverage. IMPT-PTV had larger relative differences for the target volumes compared to IMPT-Robust (the results can be seen in section 4.4). For IMPT-Robust the relative

difference is always below 3%, whereas for IMPT-PTV the maximum difference is as high as 11%. Since only 2 patients were checked this should be investigated further, but it indicates that the IMPT-Robust plans are indeed more robust against positioning uncertainties than the IMPT-PTV plans. Zaghian et al. supports these findings and stress the importance of using robust optimization for IMPT (56).

Robust evaluation of the parotid glands showed quite large differences for isocenter shifts for the right-left and the anterior-posterior directions for the two patients tested. One of the patients also showed large difference in superior-inferior shift for the right parotid gland. The differences cancelled each other out in corresponding directions, i.e a right shift of 0.5 cm cancelled out the left shift of 0.5 cm. The significance of this is therefore questionable; for each fraction the uncertainties will vary and at the end of treatment the total difference may well be close to zero. The objective functions on the parotid gland were not optimized with the robust function and this may have contributed to the large differences seen for the perturbed treatment plans.

The robust evaluation also has a shortcoming because only a limited set of uncertainty scenarios were checked. The scenarios only accounted for set up uncertainties in the x, y and z directions. In this thesis the robustness against density variation and conversion of HU numbers were not evaluated.

5.4 Field arrangement

In IMPT, the user decides the beam configuration. This thesis uses a 3 field technique: two oblique anterior and one posterior. In the beginning of the work for this master thesis several different field configurations were tried and found inadequate for the included head and neck cases. 4 and 5 field techniques had acceptable target coverage but resulted in added dose to healthy tissue compared to 3 fields. Also it was observed that is was more difficult to spare the parotid glands with additional fields.

Several studies have investigated the ideal field arrangement: van Dijk et al. found in a retrospective study that increasing the number of fields improved the sparing of healthy tissue (35). They concluded that 5 fields gave the best compromise between reduced NTCP values

and CTV coverage for perturbed plans. Kraan et al. increased the number of beam directions to evaluate the robustness of each configuration, and found that 5 or 7 beam directions were not significantly more robust than 3 (8).

5.4.1 Spot placement

Due to the use of two different range shifters, explained in section 3.2.2, the placements of the spots differ slightly for patients 1-13 and patients 18-23. For patient 18, both set ups were tested, and the spot placement can be seen in figure 5.2. In this figure the difference is obvious; when the 40 mm range shifter is used on the oblique beams the spots are placed at deeper depths than with the 75 mm range shifter. Also, the effect of the ”restrict beam function” used for patients 18-23 (along with 75 mm range shifter) is seen, as the spots are only located at the same side of the patient as the beam, figure 5.2b. Figure 5.2a shows that spots are placed on the other side as well, leading to beams traversing longer inside the patients.

A reason for using the ”restrict beam function” for protons, is that the number of Bragg peaks are fewer, and less entrance dose is given to the surrounding healthy tissue. This may translate into lower probability of late effects. This may also reduce the number of high-weight spots and fewer spots placed at ”illogical” locations. Without the restriction it was observed that spots were placed outside the target volume and also outside the patient. With the restrict beam function this seemed to be fixed, at least to some extent. Another function that may help is the use of a target margin that restrict the spot placement to a chosen value [cm] outside the target volume, but it only works in the lateral direction. This target margin can also be set to auto, which was done in this thesis, and the spot placement is then determined as a function of the average spot size at Bragg peak maximum over the target projection (30). In the newest version of RayStation (v.6), this function is expanded to allow the user to restrict the placements of spots also in the depth direction, and this may further help with the spots placement (57). This version was unfortunately not installed when this master thesis was written.

Spot size

A specification not considered in this study is the spot size. It was suggested by Stenenker et al. that smaller spot sizes reduced the parotid dose and significantly reduced the integral dose and the risk for secondary cancer (58). Later, van de Water et al. published their results

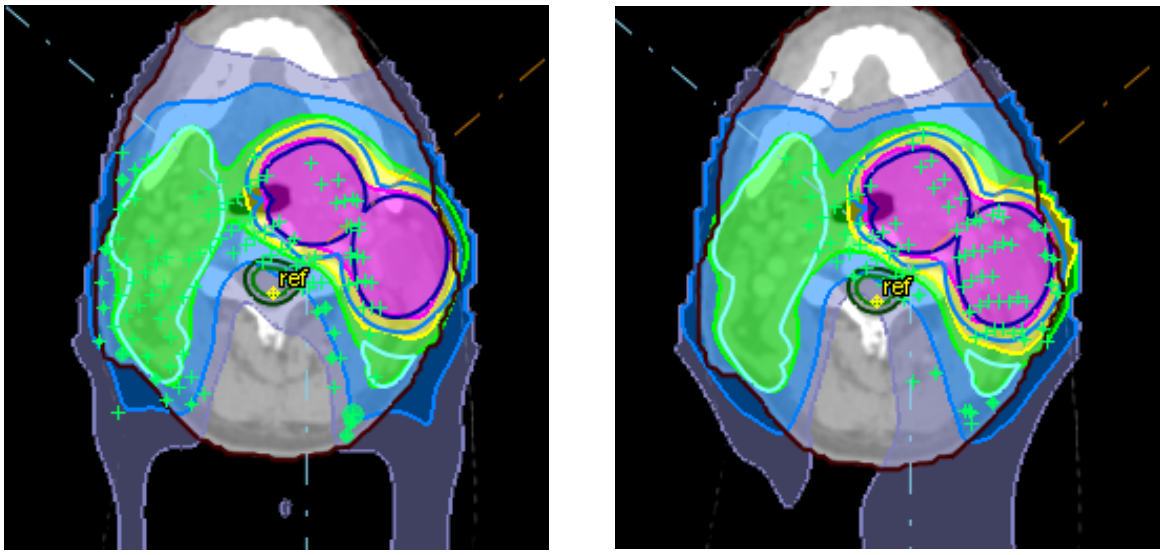

(a) 40 mm range shifter (b) 75 mm range shifter

Figure 5.2: Spot placement for the two different range shifters and beam restrictions for the 50° beam used in this master thesis.

of a treatment planning study comparing two different spot sizes (59). The authors concluded that applying a smaller spot size resulted in significantly reduced mean dose to the parotid and submandibular gland, and that this should translate into significant clinical benefit for most patients.

5.5 Dental fillings

9 of the 12 patients in this thesis have dental fillings that cause artifacts in the CT images, and Richard et al. concluded that such metal dental fillings impact tumor and tissue density (60). This will add to the uncertainties, especially for IMPT, that can degrade the quality and accuracy of the treatment plan. Jäkel and Reiss (61) investigated how the range of ion beams was affected by metal implants in the head and neck. They found that streak artifacts gave a range error of below 1%, when the beam paths avoided the metal implant, because of cancellations between high and low density regions.

If the beam path was set to go through the metal implant, the range was underestimated with about 3% (61). This 3% underestimation would mean that areas behind the implant may suffer from under-dosage. For patients in this thesis, this might reduce the tumor control probability because in some of the cases the tumors are located behind the implant with respect to the beam path. This is somewhat corrected for in patients 18-23 where the anterior, oblique beams are

restricted to only put spots on their respective sides. Verburg and Seco and Park et al. have both suggested methods to correct for metal artifacts, based on a reduction method algorithm (31) and MRI (62).

5.6 Future work

The benefit of IMPT vs VMAT, as seen in this master thesis, seems to be highly patient specific and this makes it difficult to single out subgroups. It is therefore necessary to work out efficient methods to choose the patients that benefit the most, which Langendijk et al. is in the process of doing in the Netherlands (7) with a model-based approach based on NTCP.

Others have suggested similar techniques for identifying patients who will benefit from IMPT, both from sparing healthy tissue and relating to cost. Cheng et al. developed and tested an online platform for comparing photon and proton treatments on DVHs, toxicity and cost-effectiveness (63). Löck et al. suggested an exchange of plans between centers to identify and enhance knowledge of patient assignment to photon or particle therapy (64). All of these methods have in common that both photon and proton treatment plans has to be made (either in the same center or at two different ones). Therefore Delaney et al. recently pointed out that making both VMAT and IMPT plans is time consuming and prone to bias (65). They suggest using a knowledge-based planning solution, that is using a library of created treatment plans to construct a model and predict achievable OAR DVHs for future patients.

This is research in its infancy and no such methods are tried out in this thesis. Further work could be done to assess the different methods already proposed in the literature. Work should also be done to evaluate all the possibilities of being able to select those patients that will benefit the most from proton therapy, i.e. IMPT. The cost-effectiveness of IMPT is beyond the scope of this thesis, but Blanchard et al. has discussed the possible reduction of costs associated with IMPT by reducing side effects for head and neck cancer (66).

Future work and clinical trials should be done by including more unilateral and bilateral cases, comparing them and evaluating if either one has a higher benefit from IMPT versus VMAT.

Also including more patients for the robust evaluation in addition to more set up uncertainty scenarios (combination of isocenter shifts in different directions) and changes in the density would be beneficial. More CTs could be acquired and evaluated for further investigation of optimal adaptive treatment planning for head and neck cancer, when using IMPT.

Lastly future work is necessary if a standardized IMPT field configuration is to be made for head and neck cancer. Also, spot size may be of great importance for IMPT in the future and work should be done to confirm and evaluate the possible benefits. The issue of metal artifacts due to metal dental fillings in CT should be investigated further and taken into account for clinical head and neck cancer treatment.

Chapter 6

Conclusion

IMPT for head and neck cancer was investigated and compared to VMAT for 12 oropharynx cancer patient cases. IMPT plans were made PTV-based and robust optimized. A new CT was taken halfway through the treatment to recalculate the treatment plans and evaluate the robustness of IMPT.

The IMPT plans were kept equal (or better) in terms of target dose coverage as the clinical VMAT plans. The mean parotid dose was then reduced as much as possible without losing target coverage. Compared to VMAT, IMPT reduced the mean dose to both parotid glands for 8 of 12 patients, with a corresponding reduction in the NTCP for xerostomia. Robust optimized IMPT achieved the lowest mean parotid dose and also the lowest NTCP.

A repeat CT was taken halfway through the treatment and was used to check IMPT's robustness for patient anatomy changes. The robust optimized IMPT plans were deemed the most robust: 11 of 12 patients still had adequate target coverage, whereas for PTV-based IMPT only 6 patients had target coverage. For 2 patients, perturbed dose distributions were made and the robust optimized IMPT plans were again the most robust against setup uncertainties.

This thesis shows that IMPT may be beneficial for most cases of oropharynx cancer, when considering reduced dose to the parotid glands. Robust optimized IMPT should be preferred over PTV-based IMPT. The benefit of IMPT is highly patient specific, and more work should be done to identify the patients who will benefit the most.

Bibliography

[1] I. Larsen, B. Møller, T. Johannesen, S. Larønningen, T. Robsahm, T. Grimsrud, and G. Ursin, *Cancer incidence, mortality, survival and prevalence in Norway*. 2016.

[2] C. J. v. As-Brooks and E. C. Ward, *Head and Neck Cancer : Treatment, Rehabilitation, and Outcomes*, vol. Second edition. San Diego, CA: Plural Publishing, Inc, 2014.

[3] J. Bernier, ed., *Head and Neck Cancer : Multimodality Management*. Cham: Springer International Publishing, 2016.

[4] M. R. McKeever, T. T. Sio, G. B. Gunn, E. B. Holliday, P. Blanchard, M. S. Kies, R. S. Weber, and S. J. Frank, "Reduced acute toxicity and improved efficacy from intensity-modulated proton therapy (impt) for the management of head and neck cancer.," *Chinese clinical oncology*, vol. 5, p. 54, Aug 2016.

[5] E. B. Holliday and S. J. Frank, "Proton radiation therapy for head and neck cancer: A review of the clinical experience to date," *International Journal of Radiation Oncology, Biology, Physics*, vol. 89, no. 2, pp. 292–302, 2014.

[6] T. A. van de Water, H. P. Bijl, C. Schilstra, M. Pijls-Johannesma, and J. A. Langendijk, "The potential benefit of radiotherapy with protons in head and neck cancer with respect to normal tissue sparing: a systematic review of literature.," *The oncologist*, vol. 16, pp. 366–77, 2011.

[7] J. A. Langendijk, P. Lambin, D. De Ruysscher, J. Widder, M. Bos, and M. Verheij, "Selection of patients for radiotherapy with protons aiming at reduction of side effects: The model-based approach," vol. 107, pp. 267–273, June 2013.

[8] A. C. Kraan, S. van de Water, D. N. Teguh, A. Al-Mamgani, T. Madden, H. M. Kooy, B. J. M. Heijmen, and M. S. Hoogeman, "Dose uncertainties in impt for oropharyngeal

cancer in the presence of anatomical, range, and setup errors," *International Journal of Radiation Oncology, Biology, Physics*, vol. 87, no. 5, pp. 888–896, 2013.

[9] W. Liu, X. Zhang, Y. Li, and R. Mohan, "Robust optimization of intensity modulated proton therapy.," *Medical physics*, vol. 39, pp. 1079–91, Feb 2012.

[10] D. Pflugfelder, J. J. Wilkens, and U. Oelfke, "Worst case optimization: a method to account for uncertainties in the optimization of intensity modulated proton therapy," *Worst case optimization*, vol. 53, no. 6, pp. 1689–1700, 2008.

[11] A. Fredriksson, A. Forsgren, and B. Hardemark, "Minimax optimization for handling range and setup uncertainties in proton therapy.," *Medical physics*, vol. 38, pp. 1672–84, Mar 2011.

[12] C. B. Simone, D. Ly, T. D. Dan, J. Ondos, H. Ning, A. Belard, J. O'connell, R. W. Miller, and N. L. Simone, "Comparison of intensity-modulated radiotherapy, adaptive radiotherapy, proton radiotherapy, and adaptive proton radiotherapy for treatment of locally advanced head and neck cancer," *Radiotherapy and Oncology*, vol. 101, no. 3, pp. 376–382, 2011.

[13] A. E. Aarberg, *Comparison of 3D-CRT, VMAT and Proton Therapy for Mediastinal Lymphoma*. Department of physics, NTNU, 2016.

[14] P. Mayles, A. Nahum, and J. Rosenwald, *Handbook of Radiotherapy Physics : Theory and Practice*. Independence, US: CRC Press, 2007.

[15] D. J. Thomas, "Icru report 85: fundamental quantities and units for ionizing radiation," 2012.

[16] T. A. Berman, S. S. James, and R. Rengan, "Proton beam therapy for non-small cell lung cancer: Current clinical evidence and future directions," 2015.

[17] J. S. Lilley, *Nuclear physics : principles and applications*. The Manchester physics series, Chichester: Wiley, 2001.

[18] H. Paganetti, *Proton Therapy Physics*. No. Vol. 20 in Series in Medical Physics and Biomedical Engineering, Boca Raton, FL: CRC Press, 2012.

[19] G. G. Steel, ed., *Basic clinical radiobiology*. London: Arnold, 2002.

[20] F. M. Khan, *Khan's the physics of radiation therapy*. Philadelphia: Wolters Kluwer Health, fifth edition. ed., 2014.

[21] H. Paganetti, A. Niemierko, M. Ancukiewicz, L. E. Gerweck, M. Goitein, J. S. Loeffler, and H. D. Suit, "Relative biological effectiveness (rbe) values for proton beam therapy," *International Journal of Radiation Oncology*Biology*Physics*, vol. 53, pp. 407–421, June 2002.

[22] ICRU, "Report 78," *Journal of the ICRU*, vol. 7, Dec. 2007.

[23] T. Bortfeld, *Image-Guided IMRT : Concepts and Clinical Applications*. Springer Berlin Heidelberg, 2006.

[24] Y. Nishimura, *Intensity-Modulated Radiation Therapy : Clinical Evidence and Techniques*. Springer Japan : Imprint: Springer, 2015.

[25] M. Durante and H. Paganetti, "Nuclear physics in particle therapy: a review," 2016.

[26] S. Mcgowan, N. Burnet, and A. Lomax, "Treatment planning optimisation in proton therapy," *British Journal Of Radiology*, vol. 86, no. 1021, 2013.

[27] S. J. Frank, J. D. Cox, M. Gillin, R. Mohan, A. S. Garden, D. I. Rosenthal, G. B. Gunn, R. S. Weber, M. S. Kies, J. S. Lewin, M. F. Munsell, M. B. Palmer, N. Sahoo, X. Zhang, W. Liu, and X. R. Zhu, "Multifield optimization intensity modulated proton therapy for head and neck tumors: A translation to practice," *International Journal of Radiation Oncology, Biology, Physics*, vol. 89, pp. 846–853, July 2014.

[28] R. Malyapa, M. Lowe, A. Bolsi, A. J. Lomax, D. C. Weber, and F. Albertini, "Evaluation of robustness to setup and range uncertainties for head and neck patients treated with pencil beam scanning proton therapy," *Particle Therapy Special Edition*, vol. 95, pp. 154–162, May 2016.

[29] L. Placidi, A. Bolsi, A. J. Lomax, R. A. Schneider, R. Malyapa, D. C. Weber, and F. Albertini, "Effect of anatomic changes on pencil beam scanned proton dose distributions for cranial and extracranial tumors," vol. 97, pp. 616–623, Mar. 2017.

[30] R. Laboratories, *Raystation 5 User Manual*, 2016.

[31] J. M. Verburg and J. Seco, "Ct metal artifact reduction method correcting for beam hardening and missing projections," *CT metal artifact reduction method correcting for beam hardening and missing projections*, vol. 57, no. 9, pp. 2803–2818, 2012.

[32] S. Levernes, *Volum og doser i ekstern stråleterapi - Definisjoner og anbefalinger. StrålevernRapport 2012:9.* 2012.

[33] ICRU, "Report 83," *Journal of the ICRU*, vol. 10, Apr. 2010.

[34] J. Unkelbach, T. Bortfeld, B. C. Martin, and M. Soukup, "Reducing the sensitivity of impt treatment plans to setup errors and range uncertainties via probabilistic treatment planning," *Medical Physics*, vol. 36, no. 1, pp. 149–163, 2009.

[35] van Dijk, V. Lisanne, R. J. H. M. Steenbakkers, B. ten Haken, H. P. van der Laan, A. A. van 't Veld, J. A. Langendijk, and E. W. Korevaar, "Robust intensity modulated proton therapy (impt) increases estimated clinical benefit in head and neck cancer patients," *PLoS ONE*, vol. 11, no. 3, pp. urn:issn:1932–6203, 2016.

[36] T. Inaniwa, N. Kanematsu, T. Furukawa, and A. Hasegawa, "Arobust algorithm of intensity modulated proton therapy for critical tissue sparing and target coverage," *A robust IMPT optimization against range and setup uncertainties*, vol. 56, no. 15, pp. 4749–4770, 2011.

[37] P. Lougovski, J. LeNoach, L. Zhu, Y. Ma, Y. Censor, and L. Xing, "Toward truly optimal imrt dose distribution: Inverse planning with voxel-specific penalty," *Technology in cancer research & treatment*, vol. 9, pp. 629–636, Dec. 2010.

[38] E. B. Podgorsak, ed., *Radiation oncology physics : a handbook for teachers and students*. Vienna: International Atomic Energy Agency, 2005.

[39] J. T. Lyman, "Complication probability as assessed from dose-volume histograms.," *Radiation research. Supplement*, vol. 8, pp. S13–9, 1985.

[40] G. J. Kutcher and C. Burman, "Calculation of complication probability factors for non-uniform normal tissue irradiation: the effective volume method.," *International journal of radiation oncology, biology, physics*, vol. 16, pp. 1623–30, Jun 1989.

[41] A. Niemierko, "Reporting and analyzing dose distributions: a concept of equivalent uniform dose," *Medical physics*, vol. 24, no. 1, p. 103, 1997.

[42] R. Qiuwen Wu, A. Mohan, and A. Niemierko, "Imrt optimization based on the generalized equivalent uniform dose (eud)," 2000.

[43] R. Mohan, G. S. Mageras, B. Baldwin, L. J. Brewster, G. J. Kutcher, S. Leibel, C. M. Burman, C. C. Ling, and Z. Fuks, "Clinically relevant optimization of 3-d conformal treatments," *Medical Physics*, vol. 19, no. 4, pp. 933–944, 1992.

[44] E. Hedin and A. Bäck, "Influence of different dose calculation algorithms on the estimate of ntcp for lung complications," *Journal of Applied Clinical Medical Physics*, vol. 14, no. 5, pp. 127–139, 2013.

[45] L. Feuvret, G. Noel, J.-J. Mazeron, and P. Bey, "Conformity index: a review.," *International journal of radiation oncology, biology, physics*, vol. 64, pp. 333–42, Feb 2006.

[46] J. O. Deasy, A. I. Blanco, and V. H. Clark, "Cerr: a computational environment for radiotherapy research.," *Medical physics*, vol. 30, pp. 979–85, May 2003.

[47] A. C. Houweling, M. E. P. Philippens, T. Dijkema, J. M. Roesink, C. H. J. Terhaard, C. Schilstra, R. K. Ten Haken, A. Eisbruch, and C. P. J. Raaijmakers, "A comparison of dose-response models for the parotid gland in a large group of head-and-neck cancer patients," vol. 76, pp. 1259–1265, Mar. 2010.

[48] *MATLAB version 9.1.0 (R2016b)*. Natick, MA, USA, 2016.

[49] van de Water, A. Tara, A. J. Lomax, H. P. Bijl, M. E. de Jong, C. Schilstra, E. B. Hug, and J. A. Langendijk, "Potential benefits of scanned intensity-modulated proton therapy versus advanced photon therapy with regard to sparing of the salivary glands in oropharyngeal cancer," vol. 79, pp. 1216–1224, Mar. 2011.

[50] C. Stromberger, L. Cozzi, V. Budach, A. Fogliata, P. Ghadjar, W. Wlodarczyk, B. Jamil, J. Raguse, A. Böttcher, and S. Marnitz, "Unilateral and bilateral neck sib for head and neck cancer patients," *Strahlenther Onkol*, vol. 192, no. 4, pp. 232–239, 2016.

[51] A. I. Blanco, K. S. C. Chao, I. El Naqa, G. E. Franklin, K. Zakarian, M. Vicic, and J. O. Deasy, "Dose-volume modeling of salivary function in patients with head-and-neck cancer receiving radiotherapy," vol. 62, pp. 1055–1069, July 2005.

[52] A. Jakobi, A. Bandurska-Luque, K. Stützer, R. Haase, S. Löck, L.-J. Wack, D. Mönnich, D. Thorwarth, D. Perez, A. Lühr, D. Zips, M. Krause, M. Baumann, R. Perrin, and C. Richter, "Identification of patient benefit from proton therapy for advanced head and neck cancer patients based on individual and subgroup normal tissue complication probability analysis," vol. 92, pp. 1165–1174, Aug. 2015.

[53] A. W. T. Konings, F. Cotteleer, H. Faber, P. van Luijk, H. Meertens, and R. P. Coppes, "Volume effects and region-dependent radiosensitivity of the parotid gland," vol. 62, pp. 1090–1095, July 2005.

[54] F. Albertini, E. B. Hug, and A. J. Lomax, "Is it necessary to plan with safety margins for actively scanned proton therapy?," *Is it necessary to plan with safety margins for actively scanned proton therapy?*, vol. 56, no. 14, pp. 4399–4413, 2011.

[55] P. Zhang, A. Simon, B. Rigaud, J. Castelli, J. D. Ospina Arango, M. Nassef, O. Henry, J. Zhu, P. Haigron, B. Li, H. Shu, and R. De Crevoisier, "Optimal adaptive imrt strategy to spare the parotid glands in oropharyngeal cancer.," *Radiotherapy and oncology : journal of the European Society for Therapeutic Radiology and Oncology*, vol. 120, pp. 41–7, Jul 2016.

[56] M. Zaghian, W. Cao, W. Liu, L. Kardar, S. Randeniya, R. Mohan, and G. Lim, "Comparison of linear and nonlinear programming approaches for "worst case dose" and "minmax" robust optimization of intensity-modulated proton therapy dose distributions," *Journal of Applied Clinical Medical Physics*, vol. 18, no. 2, pp. 15–25, 2017.

[57] R. Laboratories, *Raystation 6 User Manual*, 2017.

[58] M. Steneker, A. Lomax, and U. Schneider, "Intensity modulated photon and proton therapy for the treatment of head and neck tumors," *Papers from ICTR 2006. International Conference on Translational Research and Pre-Clinical Strategies in Radiation Oncology*, vol. 80, pp. 263–267, Aug. 2006.

[59] van de Water, A. Tara, A. J. Lomax, H. P. Bijl, C. Schilstra, E. B. Hug, and J. A. Langendijk, "Using a reduced spot size for intensity-modulated proton therapy potentially improves salivary gland-sparing in oropharyngeal cancer," vol. 82, pp. e313–e319, Feb. 2012.

[60] P. Richard, G. Sandison, Q. Dang, B. Johnson, T. Wong, and U. Parvathaneni, "Dental amalgam artifact: Adverse impact on tumor visualization and proton beam treatment planning in oral and oropharyngeal cancers.," *Practical radiation oncology*, vol. 5, pp. e583–8, Nov-Dec 2015.

[61] O. Jäkel and P. Reiss, "The influence of metal artefacts on the range of ion beams," *The influence of metal artefacts on the range of ion beams*, vol. 52, no. 3, pp. 635–644, 2007.

[62] P. C. Park, E. Schreibmann, J. Roper, E. Elder, I. Crocker, T. Fox, X. R. Zhu, L. Dong, and A. Dhabaan, "Mri-based computed tomography metal artifact correction method for improving proton range calculation accuracy," vol. 91, pp. 849–856, Mar. 2015.

[63] Q. Cheng, E. Roelofs, B. L. T. Ramaekers, D. Eekers, J. van Soest, T. Lustberg, T. Hendriks, F. Hoebers, H. P. van der Laan, E. W. Korevaar, A. Dekker, J. A. Langendijk, and P. Lambin, "Development and evaluation of an online three-level proton vs photon decision support prototype for head and neck cancer - comparison of dose, toxicity and cost-effectiveness," vol. 118, pp. 281–285, Feb. 2016.

[64] S. Löck, K. Roth, T. Skripcak, M. Worbs, S. Helmbrecht, A. Jakobi, U. Just, M. Krause, M. Baumann, W. Enghardt, and A. Lühr, "Implementation of a software for remote comparison of particle and photon treatment plans: Recompare," vol. 25, pp. 287–294, Sept. 2015.

[65] A. R. Delaney, M. Dahele, J. P. Tol, I. T. Kuijper, B. J. Slotman, and W. F. A. R. Verbakel, "Using a knowledge-based planning solution to select patients for proton therapy.," *Radiotherapy and oncology : journal of the European Society for Therapeutic Radiology and Oncology*, Apr 2017.

[66] P. Blanchard, A. S. Garden, G. B. Gunn, D. I. Rosenthal, W. H. Morrison, M. Hernandez, J. Crutison, J. J. Lee, R. Ye, C. D. Fuller, A. S. R. Mohamed, K. A. Hutcheson, E. B. Holliday, N. G. Thaker, E. M. Sturgis, M. S. Kies, X. R. Zhu, R. Mohan, and S. J. Frank, "Intensity-modulated proton beam therapy (impt) versus intensity-modulated photon therapy (imrt) for patients with oropharynx cancer - a case matched analysis," *Radiotherapy and Oncology*, vol. 120, no. 1, pp. 48–55, 2016.

Appendix A

Target dose coverage

Table A.1: Patient 1

ROI	cm^3	Dose/volume parameter	VMAT	IMPT-PTV	IMPT-Robust
PTV68	85	V_{95} (%)	99.90	99.55	_
		V_{105} (%)	0.00	0.00	_
PTV60	142	V_{95} (%)	99.91	99.54	_
$PTV54_{ex}$	168	V_{95} (%)	99.67	99.15	_
		V_{105} (%)	0.31	0.49	_
CTV68	40	D_{mean} (Gy)	68.03	68.05	68.18
		D_{98} (Gy)	67.28	67.44	65.69
		D_2 (Gy)	68.99	69.06	70.40
CTV60	75	D_{98} (Gy)	65.98	65.92	62.37
$CTV54_{ex}$	76	D_{mean} (Gy)	54.62	54.13	54.31
		D_{98} (Gy)	53.28	53.01	52.27
		D_2 (Gy)	58.73	56.31	56.23

Table A.2: Patient 2

ROI	cm^3	Dose/volume parameter	VMAT	IMPT-PTV	IMPT-Robust
PTV68	161	V_{95} (%)	94.69	98.33	_
		V_{105} (%)	0.00	0.02	_
PTV60	250	V_{95} (%)	96.58	98.79	_
$PTV54_{ex}$	226	V_{95} (%)	93.96	97.19	_
		V_{105} (%)	0.87	1.42	_
CTV68	83	D_{mean} (Gy)	68.10	68.21	68.06
		D_{98} (Gy)	66.91	66.94	65.83
		D_2 (Gy)	68.95	69.85	70.16
CTV60	149	D_{98} (Gy)	64.15	64.95	62.30
$CTV54_{ex}$	103	D_{mean} (Gy)	55.08	54.24	54.29
		D_{98} (Gy)	52.74	52.93	52.62
		D_2 (Gy)	63.60	56.98	56.30

Table A.3: Patient 3

ROI	cm^3	Dose/volume parameter	VMAT	IMPT-PTV	IMPT-Robust
PTV68	117	V_{95} (%)	99.29	99.38	_
		V_{105} (%)	0.02	0.00	_
PTV60	193	V_{95} (%)	99.70	99.37	_
$PTV54_{ex}$	258	V_{95} (%)	99.74	99.18	_
		V_{105} (%)	2.71	0.23	_
CTV68	60	D_{mean} (Gy)	67.97	68.05	68.23
		D_{98} (Gy)	66.97	67.10	65.79
		D_2 (Gy)	68.93	69.14	70.32
CTV60	112	D_{98} (Gy)	65.10	65.46	61.53
$CTV54_{ex}$	105	D_{mean} (Gy)	54.79	54.17	54.45
		D_{98} (Gy)	52.88	52.86	52.56
		D_2 (Gy)	59.28	57.03	56.34

Table A.4: Patient 4

ROI	cm^3	Dose/volume parameter	VMAT	IMPT-PTV	IMPT-Robust
PTV68	327	V_{95} (%)	99.43	99.52	_
		V_{105} (%)	0.02	0.02	_
PTV60	559	V_{95} (%)	99.27	99.32	_
$PTV54_{ex}$	184	V_{95} (%)	98.23	98.55	_
		V_{105} (%)	2.29	0.21	_
CTV68	153	D_{mean} (Gy)	68.21	68.01	68.12
		D_{98} (Gy)	67.33	66.48	66.25
		D_2 (Gy)	69.08	70.29	70.08
CTV60	322	D_{98} (Gy)	65.53	65.60	61.64
$CTV54_{ex}$	99	D_{mean} (Gy)	56.88	54.89	54.33
		D_{98} (Gy)	53.45	53.12	51.89
		D_2 (Gy)	64.55	59.57	56.82

Table A.5: Patient 6

ROI	cm^3	Dose/volume parameter	VMAT	IMPT-PTV	IMPT-Robust
PTV68	216	V_{95} (%)	99.04	99.55	_
		V_{105} (%)	0.19	0.12	_
PTV60	322	V_{95} (%)	99.01	99.38	_
$PTV54_{ex}$	367	V_{95} (%)	97.91	98.80	_
		V_{105} (%)	2.52	5.25	_
CTV68	122	D_{mean} (Gy)	68.69	68.00	68.02
		D_{98} (Gy)	66.56	66.91	66.18
		D_2 (Gy)	70.79	69.80	69.89
CTV60	196	D_{98} (Gy)	65.36	65.76	62.72
$CTV54_{ex}$	164	D_{mean} (Gy)	54.93	54.28	54.68
		D_{98} (Gy)	52.65	52.45	52.57
		D_2 (Gy)	59.01	58.43	56.38

Table A.6: Patient 9

ROI	cm^3	Dose/volume parameter	VMAT	IMPT-PTV	IMPT-Robust
PTV68	40	V_{95} (%)	99.61	99.89	_
		V_{105} (%)	0.00	0.65	_
PTV60	142	V_{95} (%)	98.86	98.86	_
$PTV54_{ex}$	275	V_{95} (%)	96.79	96.79	_
		V_{105} (%)	1.62	0.85	_
CTV68	11	D_{mean} (Gy)	68.55	68.14	68.00
		D_{98} (Gy)	67.75	66.50	65.93
		D_2 (Gy)	69.47	70.47	69.56
CTV60	74	D_{98} (Gy)	59.43	58.17	58.75
$CTV54_{ex}$	130	D_{mean} (Gy)	54.87	54.33	54.24
		D_{98} (Gy)	53.24	52.35	52.40
		D_2 (Gy)	59.60	57.34	56.26

Table A.7: Patient 13

ROI	cm^3	Dose/volume parameter	VMAT	IMPT-PTV	IMPT-Robust
PTV68	100	V_{95} (%)	96.31	99.58	_
		V_{105} (%)	0.08	0.00	_
PTV60	171	V_{95} (%)	98.78	99.57	_
$PTV54_{ex}$	268	V_{95} (%)	96.58	98.40	_
		V_{105} (%)	0.25	2.04	_
CTV68	52	D_{mean} (Gy)	68.07	68.15	68.34
		D_{98} (Gy)	67.01	66.93	65.98
		D_2 (Gy)	69.15	70.07	70.54
CTV60	96	D_{98} (Gy)	60.67	64.14	61.76
$CTV54_{ex}$	137	D_{mean} (Gy)	55.02	54.41	54.60
		D_{98} (Gy)	53.04	52.73	52.27
		D_2 (Gy)	60.74	57.78	57.40

Table A.8: Patient 18

ROI	cm^3	Dose/volume parameter	VMAT	IMPT-PTV	IMPT-Robust
PTV68	209	V_{95} (%)	98.44	99.42	_
		V_{105} (%)	0.00	0.01	_
PTV60	354	V_{95} (%)	98.24	99.25	_
$PTV54_{ex}$	386	V_{95} (%)	98.71	98.74	_
		V_{105} (%)	0.84	0.57	_
CTV68	100	D_{mean} (Gy)	68.05	68.22	68.12
		D_{98} (Gy)	66.66	66.97	66.04
		D_2 (Gy)	69.44	70.07	70.10
CTV60	198	D_{98} (Gy)	65.18	65.55	62.29
$CTV54_{ex}$	184	D_{mean} (Gy)	55.18	54.37	54.41
		D_{98} (Gy)	53.20	52.83	52.59
		D_2 (Gy)	60.98	58.03	56.96

Table A.9: Patient 19

ROI	cm^3	Dose/volume parameter	VMAT	IMPT-PTV	IMPT-Robust
PTV68	365	V_{95} (%)	95.94	99.04	_
		V_{105} (%)	0.03	0.02	_
PTV60	542	V_{95} (%)	96.54	99.22	_
$PTV54_{ex}$	488	V_{95} (%)	97.66	98.56	_
		V_{105} (%)	1.19	0.15	_
CTV68	210	D_{mean} (Gy)	68.61	68.28	68.78
		D_{98} (Gy)	66.96	66.64	66.93
		D_2 (Gy)	69.87	70.24	70.59
CTV60	345	D_{98} (Gy)	64.26	65.27	62.69
$CTV54_{ex}$	246	D_{mean} (Gy)	55.37	54.22	54.85
		D_{98} (Gy)	52.97	52.87	53.14
		D_2 (Gy)	63.81	57.23	56.99

Table A.10: Patient 20

ROI	cm^3	Dose/volume parameter	VMAT	IMPT-PTV	IMPT-Robust
PTV68	271	V_{95} (%)	99.54	99.59	_
		V_{105} (%)	0.01	0.00	_
PTV60	421	V_{95} (%)	99.47	99.52	_
$PTV54_{ex}$	294	V_{95} (%)	99.64	99.74	_
		V_{105} (%)	0.42	0.36	_
CTV68	143	D_{mean} (Gy)	68.15	68.02	68.31
		D_{98} (Gy)	67.06	66.26	66.29
		D_2 (Gy)	69.30	69.23	70.35
CTV60	252	D_{98} (Gy)	65.42	65.95	62.75
$CTV54_{ex}$	129	D_{mean} (Gy)	54.85	54.12	54.18
		D_{98} (Gy)	53.18	53.04	52.39
		D_2 (Gy)	61.47	56.45	56.53

Table A.11: Patient 21

ROI	cm^3	Dose/volume parameter	VMAT	IMPT-PTV	IMPT-Robust
PTV68	212	V_{95} (%)	95.84	99.34	_
		V_{105} (%)	0.00	0.00	_
PTV60	333	V_{95} (%)	96.77	99.12	_
$PTV54_{ex}$	298	V_{95} (%)	97.20	98.78	_
		V_{105} (%)	0.23	0.12	_
CTV68	112	D_{mean} (Gy)	68.15	68.05	68.07
		D_{98} (Gy)	67.09	66.79	66.45
		D_2 (Gy)	68.96	69.38	70.07
CTV60	198	D_{98} (Gy)	63.89	65.43	63.42
$CTV54_{ex}$	122	D_{mean} (Gy)	54.37	54.09	54.27
		D_{98} (Gy)	53.38	53.12	52.79
		D_2 (Gy)	56.89	55.81	56.29

Table A.12: Patient 23

ROI	**cm^3**	**Dose/volume parameter**	**VMAT**	**IMPT-PTV**	**IMPT-Robust**
PTV68	151	V_{95} (%)	99.03	99.47	_
		V_{105} (%)	0.36	0.00	_
PTV60	239	V_{95} (%)	98.76	99.18	_
$PTV54_{ex}$	250	V_{95} (%)	98.19	98.71	_
		V_{105} (%)	6.62	0.20	_
CTV68	72	D_{mean} (Gy)	68.22	68.07	68.19
		D_{98} (Gy)	66.93	66.70	66.29
		D_2 (Gy)	70.18	69.67	70.19
CTV60	135	D_{98} (Gy)	65.99	65.95	62.51
$CTV54_{ex}$	105	D_{mean} (Gy)	55.02	54.20	54.27
		D_{98} (Gy)	52.94	52.63	52.84
		D_2 (Gy)	61.52	57.31	56.17

Appendix B

Organs at risk

Mean doses [Gy] to the parotid glands for all patients. *p*-values are for VMAT vs IMPT-PTV and VMAT vs IMPT-Robust, table B.1. NTCP [%] of xerostomia for the parotid glands for all patients including difference between VMAT and IMPT plans and *p*-values for all plans, table B.2. Highest dose to medulla and medulla PRV is also shown in table B.3.

Table B.1: Mean doses [Gy] to the parotid glands for all patients.

	Right			**Left**		
Patients	VMAT	IMPT-PTV	IMPT-Robust	VMAT	IMPT-PTV	IMPT-Robust
1	4.98	0.09	0.03	24.84	23.87	23.38
2	29.46	32.79	30.28	56.80	47.75	44.33
3	47.65	36.45	32.25	24.56	22.27	20.18
4	35.79	28.10	22.16	40.41	34.12	26.30
6	24.29	25.26	20.25	33.33	26.89	26.41
9	26.09	25.01	22.19	26.28	23.66	21.17
13	26.07	25.47	18.39	25.80	25.78	20.36
18	24.37	24.72	21.63	38.90	31.47	28.95
19	25.40	25.97	25.99	45.73	32.39	30.58
20	25.00	19.08	18.12	35.56	22.23	20.14
21	25.57	16.20	17.27	28.74	24.21	24.32
23	27.18	24.43	23.71	25.72	24.32	23.53
p-value		0.0345	0.0019		0.0013	< 0.001

Table B.2: NTCP [%] of xerostomia for the parotid glands for all patients including p-values for all plans. Diff. is the absolute difference between the corresponding IMPT plan and VMAT. The p-values are for VMAT vs IMPT-PTV and VMAT vs IMPT-Robust.

	Right					**Left**				
Patient	VMAT	IMPT-PTV	(Diff.)	IMPT-Robust	(Diff.)	VMAT	IMPT-PTV	(Diff.)	IMPT-Robust	(Diff.)
1	1.44	0.63	(0.81)	0.62	(0.82)	17.50	16.02	(1.48)	15.21	(2.29)
2	25.16	31.10	(5.94)	25.91	(0.75)	85.32	68.71	(16.61)	60.71	(24.61)
3	68.95	41.88	(27.07)	32.08	(36.87)	17.02	13.58	(3.44)	10.96	(6.06)
4	40.13	23.29	(16.87)	13.57	(26.56)	51.14	35.76	(15.76)	19.57	(31.57)
6	16.53	18.28	(1.75)	11.15	(5.38)	33.68	20.82	(12.86)	19.96	(13.72)
9	19.26	17.47	(1.79)	13.33	(5.93)	19.83	15.54	(4.29)	12.14	(7.69)
13	19.46	18.57	(0.89)	9.12	(10.34)	18.87	18.86	(0.01)	11.13	(7.74)
18	16.68	17.39	(0.71)	12.86	(3.82)	47.52	30.11	(17.41)	24.84	(22.84)
19	18.45	19.40	(0.95)	19.50	(1.05)	64.33	32.59	(31.74)	28.64	(35.69)
20	17.68	9.80	(7.88)	8.76	(8.92)	39.33	13.35	(25.98)	10.79	(28.54)
21	18.57	6.83	(11.74)	8.76	(9.81)	24.66	16.72	(7.94)	16.85	(7.81)
23	21.75	17.13	(4.62)	16.00	(5.75)	18.70	16.53	(2.17)	15.38	(3.32)
p-value			0.0803		0.0153			0.0023		< 0.001

Table B.3: Highest dose [Gy] to a 0.1 cm^3 volume of the Medulla and Medulla PRV (3 mm margin). The p-values are for VMAT vs IMPT-PTV and VMAT vs IMPT-Robust.

	Medulla					**PRV**				
Patient	VMAT	IMPT-PTV	(Diff.)	IMPT-Robust	(Diff.)	VMAT	IMPT-PTV	(Diff.)	IMPT-Robust	(Diff.)
1	42.41	42.75	(0.34)	40.03	(2.38)	48.39	49.20	(0.81)	45.59	(2.80)
2	38.59	41.42	(2.83)	41.64	(3.03)	42.18	49.52	(7.34)	47.67	(5.49)
3	43.77	33.93	(9.84)	33.77	(10.00)	44.98	44.08	(0.90)	39.29	(5.69)
4	44.45	38.13	(6.32)	30.81	(13.64)	47.99	44.84	(3.15)	36.61	(11.38)
6	40.77	35.64	(5.13)	34.40	(6.37)	44.83	43.08	(1.75)	39.85	(4.98)
9	39.87	29.03	(10.84)	25.72	(14.15)	42.69	35.93	(6.76)	32.27	(10.42)
13	39.80	35.43	(4.37)	29.11	(10.69)	43.32	42.41	(0.91)	36.44	(7.18)
18	37.28	40.24	(2.96)	35.82	(1.42)	42.92	48.09	(5.17)	47.26	(4.34)
19	38.60	43.34	(4.74)	42.29	(3.69)	45.80	50.29	(4.49)	45.09	(0.71)
20	38.60	40.81	(2.21)	42.76	(4.16)	43.33	48.42	(5.09)	46.35	(3.02)
21	48.37	43.71	(4.66)	43.88	(4.49)	53.20	51.68	(1.52)	49.64	(3.56)
23	45.00	40.88	(4.12)	43.26	(1.74)	49.88	48.21	(1.67)	48.12	(1.76)
p-value			0.10		0.04			0.67		0.09

Appendix C

Perturbed treatment plans

Below are dose statistics differences between the non-perturbed plan and 6 different perturbed plans. The perturbation was equal to the CTV-PTV margin (0.5 cm) and was carried out in 6 directions shown as (x,y,z). The percent change is calculated as $\frac{\text{perturbed}-\text{original}}{\text{original}} \cdot 100\%$.

Table C.1: Percentage change of planned dose distribution to perturbed plans in 6 directions (x,y,z) for patient 6.

(a) IMPT-PTV

ROI	Dose parameter	(0.5,0,0)	(-0.5,0,0)	(0,0.5,0)	(0,-0.5,0)	(0,0,0.5)	(0,0,-0.5)
CTV54$_{ex}$	D_{98}	-3.01	-5.74	-3.53	-4.48	-0.53	-5.74
	D_2	2.67	-0.41	0.02	3.90	4.81	2.62
	D_{mean}	0.87	-1.47	-0.87	0.48	0.46	-0.28
CTV60	D_{98}	-2.24	-6.54	-12.12	-3.94	-2.90	-3.51
CTV68	D_{98}	-1.37	-2.41	-9.04	-0.91	-0.78	-2.32
	D_2	0.92	0.79	0.53	3.48	1.96	0.56
	D_{mean}	-0.07	-0.24	-0.85	0.28	0.21	-0.18
Parotid right	D_{mean}	-22.33	26.44	9.03	-7.48	1.19	1.27
Parotid left	D_{mean}	17.70	-17.55	13.69	-12.94	-0.26	2.38
Medulla	Max dose 0.1 cm^3	14.28	-6.54	-5.25	7.74	-11.56	21.55

(b) IMPT-Robust

ROI	Dose parameter	(0.5,0,0)	(-0.5,0,0)	(0,0.5,0)	(0,-0.5,0)	(0,0,0.5)	(0,0,-0.5)
CTV54$_{ex}$	D_{98}	-1.55	-1.27	-1.57	-1.23	-2.29	-1.02
	D_2	1.01	0.78	0.43	1.01	0.73	3.80
	D_{mean}	-0.16	-0.31	-0.37	-0.35	-1.24	0.79
CTV60	D_{98}	-2.52	-4.38	-5.09	-4.38	-4.08	-3.73
CTV68	D_{98}	-0.71	-0.42	-0.79	-1.01	-1.45	-0.44
	D_2	-0.30	1.85	1.42	0.06	-0.31	1.93
	D_{mean}	-0.29	0.28	0.47	-0.53	-0.69	0.41
Parotid right	D_{mean}	-23.75	30.47	12.69	-9.48	17.83	-14.22
Parotid left	D_{mean}	17.23	-12.31	14.50	-12.76	2.57	0.42
Medulla	Max dose 0.1 cm^3	7.53	-4.56	-5.49	7.65	-11.19	14.10

Table C.2: Percentage change of planned dose distribution to perturbed plans in 6 directions (x,y,z) for patient 21.

(a) IMPT-PTV

ROI	Dose parameter	(0.5,0,0)	(-0.5,0,0)	(0,0.5,0)	(0,-0.5,0)	(0,0,0.5)	(0,0,-0.5)
CTV54$_{ex}$	D_{98}	-11.07	-10.15	-9.30	-4.56	-3.12	-4.07
	D_2	8.60	4.39	0.63	10.43	2.24	5.54
	D_{mean}	0.02	-2.16	-1.55	1.59	0.57	-0.24
CTV60	D_{98}	-4.48	-10.65	-10.64	-3.36	-5.85	-2.06
CTV68	D_{98}	-4.10	-7.46	-9.63	0.07	-6.83	-1.36
	D_2	3.37	4.37	0.56	8.46	2.71	5.94
	D_{mean}	-0.66	-0.75	-2.38	2.17	-1.15	0.72
Right Parotid	D_{mean}	-26.60	42.84	16.79	-15.31	4.01	-2.22
Left Parotid	D_{mean}	37.34	-26.81	16.32	-14.50	-5.25	6.77
Medulla	Max dose 0.1 cm^3	10.75	4.30	4.64	-4.32	-12.81	17.73

(b) IMPT-Robust

ROI	Dose parameter	(0.5,0,0)	(-0.5,0,0)	(0,0.5,0)	(0,-0.5,0)	(0,0,0.5)	(0,0,-0.5)
CTV54$_{ex}$	D_{98}	-1.63	-1.80	-2.24	-1.19	0.11	-2.96
	D_2	1.78	-1.19	-0.36	2.95	2.93	0.92
	D_{mean}	0.09	-0.87	-0.81	0.70	1.11	-1.00
CTV60	D_{98}	0.05	-5.20	-4.97	-2.78	-3.37	0.39
CTV68	D_{98}	-0.86	-0.27	-2.99	-0.18	-1.31	-1.73
	D_2	0.10	1.57	-0.10	1.23	2.25	0.86
	D_{mean}	-0.43	0.25	-1.15	0.73	0.72	-0.63
Right Parotid	D_{mean}	-17.20	27.56	20.96	-17.08	6.20	-3.71
Left Parotid	D_{mean}	29.73	-20.64	17.93	-14.76	-1.56	3.62
Medulla	Max dose 0.1 cm^3	0.98	5.10	6.29	0.93	-4.54	10.94